

Probabilistic Estimation of Hidden Migrant Fatalities Along the Central Mediterranean Route

Gregor Zens*

International Institute for Applied Systems Analysis

and

Zoe Sigman

DYNAMICS, The Hertie School and Humboldt University of Berlin

March 23, 2026

Abstract

Estimating the number of migrants who die or go missing along dangerous routes such as the Central Mediterranean remains challenging as available records are incomplete. Some incidents are never documented, and fatalities associated with such unobserved incidents are absent from observed totals. We propose a Bayesian approach for probabilistic estimation of total migrant fatalities in such settings. Building on recent developments in multiple-systems estimation, we develop a time-stratified latent-class framework that accommodates missing fatality counts for unobserved incidents. We apply the method to recoded incident-level data from the *Missing Migrants Project* for the Central Mediterranean route from 2014 to 2025, encompassing 25,712 fatalities across 1,562 incidents. Our model yields 95% credible intervals of 30,426–39,172 fatalities and 2,200–2,591 deadly incidents, indicating that approximately 66%–85% of fatalities and 60%–71% of incidents are reflected in the available data. We estimate that unreported fatalities were concentrated between 2014 and 2016. Furthermore, we document that reporting likelihood increases with incident severity, implying that smaller incidents are most likely to remain undetected. While contingent on modeling assumptions and incomplete data, our method provides a broadly applicable and principled alternative to naive data adjustment methods.

Keywords: migrant mortality; multiple-systems estimation; Bayesian inference; mixture models; measurement error

*Corresponding author. Mail: zens@iiasa.ac.at.

1 Introduction

Deaths along high-risk migration routes such as the Central Mediterranean are widely acknowledged, yet systematically undercounted. Deadly incidents typically occur offshore and outside of routine observation, reporting is fragmented across institutions with different incentives and capacities, and some incidents become known only through partial information from survivors or families. As a result, observed incident records necessarily represent an incomplete subset of all fatal incidents, and recorded fatalities constitute a lower bound on true mortality.

This gap in migrant mortality data carries significant implications across historical, social, and political domains. Maintaining an accurate historical record is fundamental to quantifying the mortality risk and lethality inherent in migratory routes. Beyond historical accuracy, these metrics serve as empirical inputs for evidence-based policymaking. More robust estimates allow for more rigorous monitoring and evaluation of policy impacts – including search-and-rescue operations – and enable comparative analyses of how mortality risks fluctuate across different geographic routes, time periods, and border policy regimes. Furthermore, improved methodology for documenting migrant fatalities directly supports the monitoring of the *United Nations (UN) Sustainable Development Goal Target 10.7*, which advocates for safe, orderly, and responsible migration through well-managed policies.

From a statistical perspective, the central challenge in estimating fatalities at sea is that *both* the number of fatal incidents and the fatality counts associated with missed incidents are unobserved. However, most methods in the capture–recapture literature focus primarily on estimating the number of missing *incidents* (or individuals) and do not directly target additional unobserved *marks* of the missing incidents, in our case the mortality burden attributable to incidents that were never recorded.

We propose a Bayesian approach to estimate total migrant fatalities in such settings, which explicitly accounts for unobserved incidents and the fatality counts associated with them. The key methodological idea is to augment latent class models for multiple systems analysis with an additional mechanism to account for unobserved fatalities. Our model allows for complex dependencies between fatality counts and capture probabilities, as the number of fatalities associated with an incident may impact the likelihood of reporting. The model further allows for flexible dependence structures among the reporting sources. Finally, the proposed mixture formulation explicitly accounts for strata in the data, accommodating the fact that the underlying reporting and fatality patterns may vary across time periods.

We apply the model to manually recoded incident-level data obtained from the *Missing Migrants Project* (MMP) database maintained by the *International Organization for Migration* (IOM) and investigate migrant mortality along the Central Mediterranean route from February 2014 to December 2025. Our main findings can be summarized as follows. First, the baseline model specification yields a 95% credible interval of 30,426 to 39,172 fatalities (about 7–9 per day) and 2,200 to 2,591 deadly incidents. Compared to the 25,712 fatalities (about 6 per day) and 1,562 incidents recorded in the MMP data, this indicates that the available records capture a majority of the mortality burden – approximately 66% to 85% of total fatalities and 60% to 71% of all fatal incidents. However, a substantial share of incidents and fatalities still goes undocumented. Second, our results indicate that the absolute number of unobserved fatalities was likely concentrated between 2014 and 2016. In addition, while aggregate reporting probabilities appear relatively constant over time, this stability may mask more complex underlying dynamics combining increasing surveillance capacities for large events and a steady decline in the average number of fatalities per incident. Third, we find that the average reporting likelihood increases with incident severity, implying that smaller incidents are the most likely to go undocumented.

1.1 Related Literature and Contributions

The proposed methodology builds on a long tradition of capture–recapture and multiple-systems analysis techniques, particularly with respect to frameworks developed within human rights and public policy contexts (Lum et al. 2013, Bird & King 2018, Manrique-Vallier et al. 2022). These techniques have been successfully applied to estimate the number of casualties in armed conflicts (Ball et al. 2002, Lum et al. 2010, Manrique-Vallier et al. 2013, 2019, Dahab et al. 2025) and to quantify the prevalence of modern slavery (Silverman 2020). Estimates based on such methods have also served as supporting evidence in war crime tribunals (Ball & Asher 2002). Historically, these approaches have their roots in ecology, where they are widely used to estimate, e.g., animal population sizes; for a comprehensive overview, see Amstrup et al. (2010).

Existing approaches for estimating the size of hidden populations vary in detail and complexity. However, they all fundamentally rely on analyzing inclusion patterns across observations to estimate the probability of non-observation, and by extension the number of unobserved individuals or incidents. The majority of human rights applications utilize frameworks developed for multiple overlapping lists, including log-linear models (e.g., Ball et al. 2002, Silverman 2020), potentially combined with model averaging ideas (e.g., Madigan & York 1997). An overview is provided in Manrique-Vallier et al. (2013). An approach closely related to the present work is Manrique-Vallier (2016) who proposes to integrate latent class modeling with Dirichlet process mixtures. More recent methodological work in this realm has focused on sparse capture patterns and the resulting inferential challenges (Johndrow et al. 2019, Chan et al. 2021), and bootstrapping for uncertainty quantification (Silverman et al. 2024).

Most existing methods focus on estimation at the level of individuals or single occurrences – the typical unit of observation in this field – with less emphasis on joint modeling of incidents and their associated *marks* (in our case, fatalities). However, marked incidents represent the

most natural unit of observation in available data sources on migrant fatalities at sea, where deaths are often clustered around vessel failure. To our knowledge, only [Farcomeni \(2022\)](#) addresses this in a related context, estimating migrant fatalities on European borders using a regression-based approach rooted in single-source capture–recapture methodology. While this represents a significant step toward principled statistical inference in such settings, it relies on assumptions that are restrictive, and particularly so within the Central Mediterranean context. First, the method treats reporting sources as independent, even though lists are often operationally linked. For instance, reports of international organizations may rely on official records, while media reports may echo other outlets. Second, the approach does not directly facilitate information sharing across strata, such as years, potentially destabilizing inference in the presence of substantial variations in surveillance intensity and operational capacity across different periods. Third, the method is heavily model-based, relying on the selection of a single best specification within a generalized linear model setting. These limitations motivate the development of methods capable of accommodating source dependence while providing greater flexibility and robustness for stratified settings.

Our contribution to this literature is twofold. First, from a statistical perspective, we develop a Bayesian framework for multiple systems analysis for marked incidents, capable of estimating posterior distributions for both the total number of incidents and any functionals of interest regarding the unreported marks. We also derive a posterior simulation algorithm to estimate the model. Second, in the context of studying migrant mortality, we conduct an in-depth analysis of the Central Mediterranean route, leveraging recoded incident-level data from the MMP covering the period 2014–2025. We produce probabilistic estimates of total mortality and the implied undercount relative to recorded totals. In supplementary analyses, we combine these estimates with additional assumptions and auxiliary data to explore plausible ranges for mortality risk per crossing attempt in this context.

The remainder of the paper is structured as follows. Section 2 describes the data, scientific questions, and key challenges when working with observed incident records in this context. Section 3 presents the model, prior specification, and posterior simulation approach. Section 4 presents our analysis of migrant deaths en route in the Central Mediterranean from 2014 to 2025. Section 5 concludes with a discussion of limitations and directions for future research. Additional simulation experiments and further details are provided in the supplementary material.

2 Data and Scientific Questions

Our analysis utilizes incident-level records from the MMP database managed by the IOM, which tracks deaths and disappearances of transiting migrants ([International Organization for Migration 2026](#)). The MMP is widely acknowledged as the most comprehensive global inventory of migrant fatalities. It covers incidents involving at least one fatality. We extracted all such records regarding the Central Mediterranean route available as of March 12, 2026, and restrict our sample to the time period from January 1, 2014 to December 31, 2025.

The MMP distinguishes between (i) *individual incidents*, (ii) *cumulative incidents* that aggregate incidents over extended periods, and (iii) *split incidents* representing entries where fatalities associated with the same event are recorded separately. We restrict attention to records classified as individual or split incidents, as cumulative incidents typically cover longer time periods and do not refer to single incidents. Related split entries are merged into a single parent incident. This yields a set of 1,562 temporally localized incidents with well-defined incident-level characteristics that occurred between February 17, 2014 and December 30, 2025.

For each incident, the outcome of interest is the reported total number of people *dead or missing*. We refer to this count throughout as *fatalities*. We define *missing* and *dead* according

to the definitions utilized by the MMP.¹ In the context of the Central Mediterranean Route, *missing* refers to the number of migrants who are reported by eyewitnesses to have been onboard a shipwrecked vessel and are assumed to have died, but whose remains have not been recovered. *Dead* refers to those migrants who have died and whose remains have been recovered. After data processing, the total fatality count in the data is 25,712.²

In accordance with the MMP’s inclusion criteria, the data analyzed here exclude deaths that occur when migrants are not in transit, e.g., in formal or informal camps or detention centers, work-related deaths of migrant workers, and deaths of migrants who have reached their destination country or have settled in a destination for more than two weeks. They also exclude reports of those who have gone missing during migration, but whose deaths cannot be assumed, e.g., those people who have lost contact with loved ones for unverifiable reasons, such as detention. Our analysis should be interpreted accordingly as referring only to the population of migrants who have died during transit.

2.1 List Creation

For each incident in the database, the MMP team collects a set of *information sources* which have reported on a given incident. We classify each unique information source string in the MMP data into one of four categories representing four surveillance systems with relatively distinct coverage, dynamics, and capabilities. The first category encompasses sources originating directly from the UN system and other intergovernmental or international organizations, including reports from the IOM itself, the *UN High Commissioner for Refugees*, and related bodies. The second category consists of official governmental sources, such as coast guard agencies, national ministries, and other state institutions. The third category includes non-governmental organizations and civil society actors, ranging from search-and-

¹See <https://missingmigrants.iom.int/methodology> (accessed Feb. 17, 2026).

²The MMP updates its data regularly. Hence, future incident and fatality counts may vary.

Raw source string (MMP)	UN/IGO	Official	NGO/Hum.	Media
IOM Libya, Lana News	1	0	0	1
Ansa, UNHCR Lampedusa	1	0	0	1
Sea Punks	0	0	1	0
IOM Libya, Pakistan PM Shehbaz Sharif	1	1	0	0
RESQSHIP, EFE	0	0	1	1

Table 1: Examples of information source classification and derived capture indicators. Each raw source string in the MMP data is coded into binary inclusion indicators for four derived reporting systems (UN/IGO, Official, NGO/Humanitarian, Media).

rescue operations to advocacy groups and humanitarian organizations. The fourth category comprises media sources, including both traditional news outlets and aggregation services.

We adopt these relatively broad groupings to balance two competing considerations. On the one hand, finer distinctions – for instance, separating local from national or international media – would yield more lists and more homogeneous reporter categories, but risk producing sparse and highly correlated lists. On the other hand, excessively coarse categories would obscure meaningful differences in reporting behavior. Our four-category scheme aims to identify source types that function as relatively independent observation and surveillance systems.

Tab. 1 presents examples of our coding logic, illustrating how specific source strings map to the four categories. Although tedious, coding these source strings is mostly straightforward. However, certain cases unavoidably require judgment calls. For instance, *ReliefWeb* is operated under the *UN Office for the Coordination of Humanitarian Affairs* but functions primarily as an aggregator of content from diverse origins, including both UN agencies and independent news organizations. We classify such online aggregators as media sources, prioritizing their functional role over their institutional affiliation. Although no classification scheme can

be entirely unambiguous, we have aimed for a procedure that is conservative, internally consistent, and reproducible.³

2.2 Benefits and Limitations of the Meta-Observer Approach

It is important to acknowledge that the four reporter categories used here do not constitute independently operating “lists” in the classical capture–recapture sense. Rather, they are defined by recoding information sources as recorded by a *meta-observer* – here, the MMP team – which collects and verifies reports from multiple surveillance systems. A key advantage of this recoding approach is that it enables us to model correlations between reporters (and, eventually, fatality marks) using ideas from multiple-systems analysis. This is crucial, as, for example, media coverage may draw on government press releases, inducing positive dependence between those two capture systems. If such positive dependence is ignored, hidden population estimates are likely biased.

A central caveat of this approach, however, is that the *meta-observer* may introduce bias in how it aggregates information from the underlying data generators. While it is plausible to assume that the IOM observation process credibly spans all four surveillance systems – and that incidents recorded in the database were indeed reported by the stated sources – it may also occur that not all sources are consistently documented. For instance, if an incident enters the database via the UN system, an additional media report might not always be recorded even if it existed. Under this perspective, non-reporting of a list is subject to uncertainty. That is, the absence of a source label does not necessarily imply that the source failed to report the event. By contrast, sources that *are* recorded in the MMP system correspond to reports that were verified and documented by the MMP team prior to inclusion.

³Zoe Sigman previously served on the MMP data collection team for the Central Mediterranean, which informed various aspects of the coding and modeling decisions described in this paper.

That said, in the context of migrant mortality en route, a *meta-observer* structure of this kind is nearly always the only feasible – and typically also the best – available data source. As a result, alternative approaches face the same limitation (e.g., [Farcomeni 2022](#)). The relatively broad capture systems we operationalize do, however, lend our approach a certain degree of robustness. For instance, it is more plausible that the MMP team captures *any* media report on a given incident than that they capture *every* such report. In our analyses below, we assume that the MMP retrieval process is approximately comprehensive with respect to the four surveillance systems. We revisit this assumption in [Sec. 5](#), where we highlight sources of bias and avenues for future work, including targeted audits of individual incidents and model extensions that explicitly account for uncertainty in source recording.

2.3 Research Questions

Drawing on the dataset described above, we address three primary research questions. First, what is the total number of migrant fatalities and deadly incidents on the Central Mediterranean route between 2014 and 2025? Second, how do these figures evolve over time, specifically regarding annual trends and intra-year seasonal patterns? Third, what is the relationship between the severity of an incident and its probability of being captured by surveillance systems?

Each of these questions requires knowledge about the full event process, including incidents and fatalities that are not observed in any list. Our strategy for answering these questions is to build a fully probabilistic estimation framework that imputes both missing incidents and their fatality counts in the estimation process. To motivate some key modeling choices, the next subsection reports some descriptive characteristics of the data that we will explicitly take into account when introducing the statistical modeling framework in [Sec. 3](#).

2.4 Empirical Stylized Facts

We begin by describing basic patterns regarding fatalities and incidents in the reported data (Fig. S3). Both the mean and the variance of the fatality distribution decline over the study period. In 2014, the average number of fatalities per incident is almost 20, decreasing to less than 5 in 2025. Similarly, total reported fatalities decrease from a peak of 4,572 in 2016 to 1,286 in 2025. Overall, the distribution of fatalities is heavily right-skewed, with 35% of incidents including only a single fatality. Across the full sample, the mean is 16.5 fatalities per incident, while the maximum corresponds to an event with 1,022 reported fatalities on April 18, 2015.

Conditional on an incident being observed, the UN/IGO list exhibits the highest average capture rate (72%), followed by the media (30%), NGOs and humanitarian partners (17%), and official sources (11%).⁴ Reporting patterns vary substantially across years (Fig. S4). In 2014–2015, the media list is the strongest source, while the UN/IGO list contributes relatively little; over time, this relationship reverses. Pairwise reporting dynamics also change substantially – for example, the UN/IGO–official pair exhibits a positive trend over the years. These patterns partially reflect the methods of the MMP team, which relied primarily on media reports and disembarkation reports from IOM Italy until 2017. After 2017, there was a shift towards more reports from NGOs and other IGOs, the initiation of reports from IOM Libya, as well as a more dedicated staffing for the MMP team.

Finally, the data indicate a complex marginal relationship between incident severity and reporting patterns (Fig. S4). For instance, the UN/IGO list exhibits a U-shaped pattern. The other lists show similarly nuanced behavior. For example, the media list has comparatively low reporting probabilities for the smallest incidents, while official sources report the largest incidents less frequently. Importantly, because these patterns are aggregated over the entire

⁴Counts of incidents for all 15 observed reporting patterns are provided in Supplementary Tab. S2.

study period, they may reflect temporal shifts in reporting practices and should thus be interpreted with caution.

Taken together, these stylized facts imply a minimum set of three requirements for a model capable of addressing the research questions outlined above. First, the model must allow for time-stratified inference for both the mark distribution and reporting patterns.⁵ Second, the model should accommodate potentially complex relationships between reporters, as well as between fatalities and reporters, that may also vary over time. Third, the model must reflect a potentially highly skewed fatality distribution. In Sec. 3, we develop a probabilistic model that addresses these challenges jointly.

3 Statistical Methodology

We consider a population of incidents partitioned into G mutually exclusive strata (e.g., time periods or geographic regions). Let N_g denote the unknown total number of incidents in stratum $g \in \{1, \dots, G\}$. We observe a subset of these incidents through R reporting systems. For each observed incident i , we record its stratum indicator $h_i \in \{1, \dots, G\}$, a reporting pattern $\mathbf{s}_i = (s_{i1}, \dots, s_{iR}) \in \{0, 1\}^R$ with $s_{ij} = 1$ if system j reported incident i (and 0 otherwise), and a positive mark $y_i \in \mathbb{R}^+$ measuring incident magnitude. In the present application, y_i is the reported fatality count and thus takes values in \mathbb{N}_+ . We also define the log-mark $x_i = \log(y_i)$. The observed dataset contains m incidents and is *zero-truncated* by construction, since incidents that are not reported by any system (i.e., with $\mathbf{s}_i = \mathbf{0}$) are unobserved. The analysis targets, for each stratum g , both the total number of incidents and the total mark sum. Writing m_g for the observed number of incidents in stratum g and n_{0g}

⁵See also <https://hrdag.org/2013/03/20/mse-stratification-estimation/> (accessed Feb. 9, 2026) on the importance of stratification in multiple systems analysis.

for the (unknown) number of unobserved incidents in that stratum, we have

$$N_g = m_g + n_{0g}. \quad (1)$$

The total mark sum – in our case, the total fatality count – in stratum g is

$$Y_g^{\text{tot}} = \underbrace{\sum_{i \in \mathcal{O}_g} y_i}_{\text{observed}} + \underbrace{\sum_{\ell=1}^{n_{0g}} y_{0g\ell}}_{\text{unobserved}}, \quad (2)$$

where \mathcal{O}_g denotes the set of observed incidents in stratum g , and $y_{0g\ell}$ is the (unknown) mark of the ℓ -th unobserved incident in stratum g . For each stratum g , the number of unobserved incidents n_{0g} is treated as a random variable. We assume the total population N_g in stratum g follows a Poisson model $N_g \sim \text{Poisson}(\lambda_g)$ with intensity λ_g .

3.1 Stratified Mark-Augmented Latent Class Model

Motivated by the success of latent class models for multiple systems analysis ([Manrique-Vallier 2016](#)), we account for unobserved heterogeneity, as well as list–list and list–mark dependencies, using a Bayesian latent class mixture model. We assume there exist K latent clusters of incidents. Let $z_i \in \{1, \dots, K\}$ be the latent cluster assignment for incident i . Within cluster k , captures are independent Bernoulli events. The probability that incident i is captured by list j is p_{kj} . The probability of observing the capture pattern \mathbf{s}_i is thus

$$P(\mathbf{s}_i \mid z_i = k, \mathbf{p}_k) = \prod_{j=1}^R p_{kj}^{s_{ij}} (1 - p_{kj})^{1-s_{ij}}, \quad (3)$$

where $\mathbf{p}_k = (p_{k1}, \dots, p_{kR})$. Consequently, the probability that an incident in cluster k remains completely unobserved is $q_k = \prod_{j=1}^R (1 - p_{kj})$. To accommodate potentially skewed mark densities, we assume log-marks follow a cluster-specific Gaussian distribution:

$$x_i \mid z_i = k \sim \mathcal{N}(\mu_k, \sigma_k^2). \quad (4)$$

A practical implication of this specification is that the incident mark is modeled as a positive continuous quantity, even though fatalities are observed as integer counts. We adopt this

continuous approximation for computational tractability and to allow flexible modeling of the highly skewed mark distribution. Accordingly, posterior summaries for total fatalities should be interpreted as estimates of the total fatality burden rather than as an exact reconstruction of an integer-valued latent count process. In practice, this distinction is negligible at the aggregate level considered here, but it implies a modest support mismatch between the model and the underlying data-generating process. We return to this issue in the discussion.

The parameters of these clusters are shared across all strata to facilitate information sharing and stability of the model. To allow for stratum-specific inference, we assume the mixing proportions of the mixture model vary by stratum. Hence, the latent cluster assignments are drawn from a stratum-specific discrete distribution. For an incident in stratum g , we have

$$P(z_i = k \mid h_i = g) = \pi_{gk}, \quad \text{with } \sum_{k=1}^K \pi_{gk} = 1. \quad (5)$$

While we assume conditional independence of capture events and marks within each cluster – a local independence assumption – the marginal distribution induced by the mixture allows for rich and complex dependencies between lists and marks. By averaging over K distinct clusters, the model effectively captures the correlation structures present in the aggregate data (McLachlan & Peel 2000, Hagenaars & McCutcheon 2002, Frühwirth-Schnatter 2006, Manrique-Vallier 2016).

Beyond providing a flexible approach for density estimation, the latent class formulation reflects the operational realities in the context of the Central Mediterranean route. Here, latent classes naturally represent unobserved heterogeneity arising from complex environmental and logistical factors that simultaneously drive incident lethality and the likelihood of documentation. For instance, incidents occurring deep within the Libyan Search and Rescue zone or during severe weather conditions frequently exhibit both higher fatality rates due to delayed rescue and lower detection probabilities by European official or media sources. Similarly, the type of vessel involved – ranging from fragile rubber dinghies to large, densely

packed fishing boats – creates distinct casualty and reporting signatures. While the capsizing of a large vessel may trigger a multi-agency response that activates multiple surveillance systems, sinkings involving smaller vessels may remain largely invisible, becoming known only through survivor testimonies collected by humanitarian agencies. By probabilistically segmenting incidents into latent clusters, our model explicitly accounts for these overlapping, unrecorded dynamics. This allows the framework to capture the dependence between incident severity and reporting patterns without requiring granular covariate data, which is frequently missing or entirely unobservable, even for known incidents.

The decision to hold cluster-specific parameters constant across strata while allowing the mixture weights (π_{gk}) to vary is driven by two main considerations. First, from a statistical and computational perspective, it is a parsimonious choice that allows the model to learn a shared “dictionary” of latent components. By sharing the component parameters across strata, the model borrows strength from the entire dataset. At the same time, the stratum-specific weights allow the model to flexibly turn specific clusters “on” or “off” in any given stratum, avoiding potential overparameterization due to estimating entirely separate models per stratum. Second, from an application perspective, this structure accommodates a wide range of real-world dynamics. It allows certain incident “archetypes” – for instance low-visibility, localized rubber dinghy deflations – to be persistently present across all strata. Simultaneously, other archetypes can fluctuate in prevalence, emerge as highly stratum-specific events, or even split into distinct components – for instance, if reporting systems become more adept at documenting high-fatality incidents in later years. Consequently, the proposed latent class formulation effectively captures both persistent, long-term surveillance patterns and transient, period-specific shifts.

In principle, one could alternatively “expand” the incident-level data by replicating each incident’s capture pattern once per reported fatality (e.g., an incident with 5 fatalities

yields 5 identical rows) and apply standard capture-recapture methodology. This would effectively treat fatalities as independent observational units with the same list-inclusion pattern, thereby reweighting the likelihood toward high-fatality incidents and implicitly assuming within-incident independence and homogeneous capture across deaths. Because our four lists are best interpreted as incident-level reporters (rather than individual-level registries), such expansion constitutes pseudo-replication, can distort estimation of capture probabilities, and may understate uncertainty. We therefore prefer to model fatalities as an incident mark jointly with the capture pattern, which preserves the correct observational unit and allows detection to depend on incident severity.

3.2 Prior Elicitation

We employ a sparse finite mixture approach (Malsiner-Walli et al. 2016) to flexibly infer both the number of active clusters and their associated weights. The key ingredient is a prior on the mixture weights π_g that induces *sparsity*, such that only a small subset of the K available components is active *a posteriori*. This allows the effective number of mixture components required to represent dependence patterns in the data to be treated as an unknown quantity and learned within the estimation procedure. Rather than fixing a single number of active clusters, this method directly accounts for the uncertainty across the true number of clusters. Closely related ideas motivate the Dirichlet process mixture specification used by Manrique-Vallier (2016). We expect broadly similar results under either mixture construction, since recent work suggests that the distinction between sparse finite and Dirichlet process mixtures is typically less influential than the choice of within-model prior specification (Frühwirth-Schnatter & Malsiner-Walli 2019). The full hierarchical prior structure we use is specified as follows:

$$\boldsymbol{\pi}_g \mid \alpha_g \sim \text{Dirichlet}\left(\frac{\alpha_g}{K}, \dots, \frac{\alpha_g}{K}\right), \quad (6)$$

$$\alpha_g \sim \text{Gamma}(a_\alpha, b_\alpha), \quad (7)$$

$$p_{kj} \sim \text{Beta}(a_p, b_p), \quad (8)$$

$$\sigma_k^2 \sim \text{Inv-Gamma}(c_0, C_0), \quad (9)$$

$$\mu_k \sim \mathcal{N}(m_0, s_0^2), \quad (10)$$

$$\lambda_g \sim \text{Gamma}(a_\lambda, b_\lambda). \quad (11)$$

The concentration parameters α_g are estimated from the data, allowing the model to adapt the effective model complexity per stratum. Throughout, we utilize the following baseline hyperparameter choices. We set the upper bound on the number of clusters to $K = 100$, large enough to ensure it does not constrain the posterior distribution of active components heavily. For the capture probabilities, we select $a_p = b_p = 1$, implying a uniform prior on $[0, 1]$ that assumes no strong prior knowledge regarding the sensitivity of the reporting lists. For the cluster-specific mark distributions, we use data-informed priors centered in the region supported by the observed data. Specifically, we set m_0 to the sample mean of the observed log-marks and s_0^2 to the corresponding sample variance. For the cluster variances, we set $c_0 = 4$, which implies a prior with finite mean and variance, and choose $C_0 = 1$. These choices are weakly informative on σ_k^2 and allow for smoother estimates of the relationship between reporting and log marks. They are also motivated by a certain numerical sensitivity of the model to prior specification for the Gaussian components. In particular, the induced lognormal distribution can exhibit extremely heavy tails if the priors on μ and σ^2 are too diffuse. The present setting remains flexible – the prior predictive distribution comfortably covers the observed range – while avoiding unrealistically large tail mass that destabilizes the posterior simulation algorithm.

To govern the sparsity of the finite mixture, we place a $\text{Gamma}(1, 1)$ prior on the concentration parameters α_g . For the population intensity λ_g , we employ an improper Jeffreys-type prior by setting $a_\lambda = 0.5$ and $b_\lambda = 0$. In the course of the data analysis in Sec. 4, we will explicitly explore the sensitivity of our results to several of these hyperparameter choices.

3.3 Posterior Inference

We explore the posterior distribution using a Gibbs sampler with data augmentation (Tanner & Wong 1987). Each sampling iteration alternates between (i) imputing the unobserved auxiliary data (the cluster membership of the observed data, as well as the size, cluster memberships, and marks of the hidden population) and (ii) updating model parameters given the observed data and the current imputations.

Updating latent auxiliary variables. For each observed incident $i \in \mathcal{O}_g$, we draw its latent cluster label $z_i \in \{1, \dots, K\}$ from a categorical distribution with probabilities proportional to the product of the stratum-specific weight, the likelihood of the reporting pattern, and the likelihood of the log-mark:

$$P(z_i = k \mid \cdot) \propto \pi_{gk} \left[\prod_{j=1}^R p_{kj}^{s_{ij}} (1 - p_{kj})^{1-s_{ij}} \right] \phi(x_i \mid \mu_k, \sigma_k^2), \quad (12)$$

where $\phi(\cdot)$ denotes the Gaussian density.

To account for incidents that are missed by all reporting systems, we augment the state space with an unobserved count n_{0g} in each stratum. We first update the stratum intensity λ_g from its Gamma full conditional,

$$\lambda_g \mid \cdot \sim \text{Gamma}(a_\lambda + m_g + n_{0g}, b_\lambda + 1), \quad (13)$$

and then sample the number of missed incidents using Poisson thinning. Let $p_{0g} = \sum_{k=1}^K \pi_{gk} q_k$ denote the marginal probability that an incident in stratum g is missed entirely, where q_k is

the probability of the all-zero reporting pattern under cluster k . We draw

$$n_{0g} \mid \cdot \sim \text{Poisson}(\lambda_g p_{0g}), \quad (14)$$

and allocate the missed incidents to clusters via

$$(n_{0g1}, \dots, n_{0gK}) \sim \text{Multinomial}\left(n_{0g}, \frac{\pi_{g1} q_1}{p_{0g}}, \dots, \frac{\pi_{gK} q_K}{p_{0g}}\right). \quad (15)$$

We then impute log-marks for the currently unobserved incidents assigned to cluster k by drawing n_{0gk} latent marks $x \sim \mathcal{N}(\mu_k, \sigma_k^2)$, and combine these draws with the observed $\{x_i : z_i = k\}$ to obtain a complete set of log-marks for cluster k .

Updating parameters. Given the observed assignments and the augmented counts, parameters are updated using standard conjugate steps. Let \mathcal{I}_k denote the set of indices for all incidents currently assigned to cluster k , comprising both the observed incidents and the indices of the augmented unobserved incidents in cluster k . The total number of incidents in cluster k is $N_k = |\mathcal{I}_k|$.

The concentration parameter α_g has no closed-form full conditional and is updated with an adaptive Metropolis–Hastings step using normal proposals on the log scale. Writing N_{gk} for the total number of incidents assigned to cluster k in stratum g , the mixture weights are updated via

$$\boldsymbol{\pi}_g \mid \cdot \sim \text{Dirichlet}\left(\frac{\alpha_g}{K} + N_{g1}, \dots, \frac{\alpha_g}{K} + N_{gK}\right). \quad (16)$$

Capture probabilities are shared across strata. Thus, each p_{kj} is updated from its Beta full conditional using the complete set of assignments. Since unobserved incidents are by definition missed by all systems, we have $s_{ij} = 0$ for all augmented incidents and the full conditional is

$$p_{kj} \mid \cdot \sim \text{Beta}\left(a_p + \sum_{i \in \mathcal{I}_k} s_{ij}, \quad b_p + \sum_{i \in \mathcal{I}_k} (1 - s_{ij})\right). \quad (17)$$

The Gaussian mark parameters (μ_k, σ_k^2) are updated via standard conjugate updates:

$$\sigma_k^2 \mid \cdot \sim \text{Inv-Gamma} \left(c_0 + \frac{N_k}{2}, \quad C_0 + \frac{1}{2} \sum_{i \in \mathcal{I}_k} (x_i - \mu_k)^2 \right), \quad (18)$$

$$\mu_k \mid \cdot \sim \mathcal{N}(\hat{m}_k, \hat{V}_k), \quad (19)$$

where the posterior mean and variance are given by

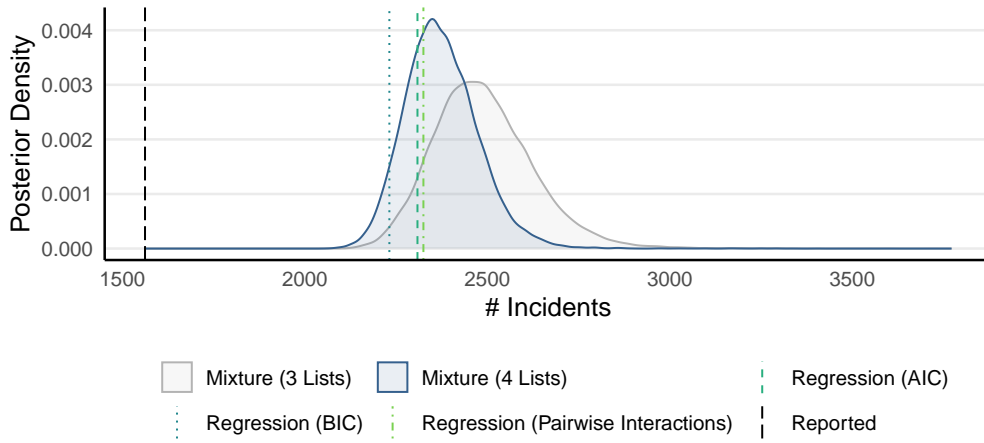
$$\hat{V}_k = \left(\frac{1}{s_0^2} + \frac{N_k}{\sigma_k^2} \right)^{-1} \quad \text{and} \quad \hat{m}_k = \hat{V}_k \left(\frac{m_0}{s_0^2} + \frac{\sum_{i \in \mathcal{I}_k} x_i}{\sigma_k^2} \right). \quad (20)$$

Additional details on the MCMC algorithm and the associated data-augmentation scheme are provided in the supplementary material (Sec. S1), where we also present a simulation study (Sec. S2). In our simulation experiments, we evaluate the proposed model and sampler across a range of data-generating processes and compare performance to several competing approaches, from naive estimators to regression-based methods in the spirit of Farcomeni (2022), which we adapt to multi-list settings in Sec. S2. The results show that our approach typically outperforms these approaches and yields accurate inference for both the total number of incidents and total fatalities, with well-calibrated posterior quantiles.

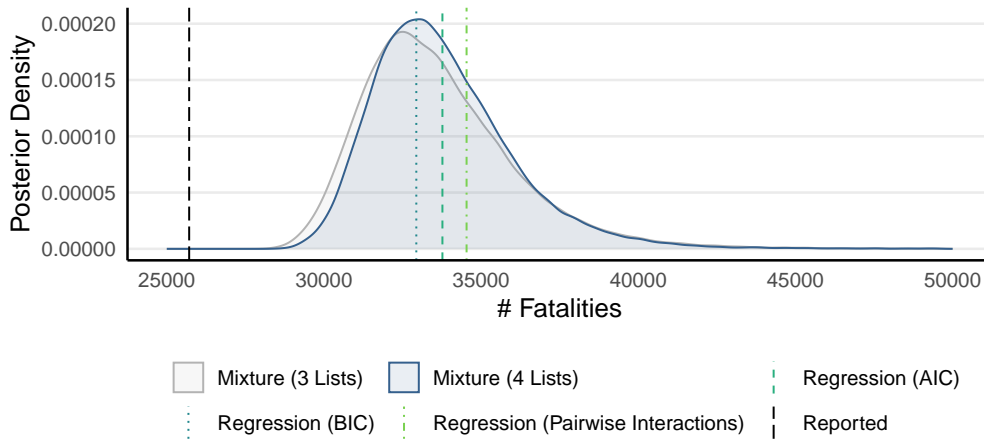
4 Results

All presented results are based on 250,000 retained posterior draws, obtained after discarding an initial burn-in of 25,000 iterations and thinning the remaining chain by a factor of six. MCMC convergence is generally satisfactory; see the trace plots in Fig. S5 in the supplementary material.

Incident and Fatality Estimates. Fig. 1 summarizes our primary results, displaying the estimated posterior densities for both the total number of incidents and fatalities. Black dashed lines represent the number of incidents and fatalities reported in the MMP data as respective lower bounds. Our preferred baseline specification, stratified by year, is shown in



(a) Posterior distribution of the total number of incidents.



(b) Posterior distribution of the total number of fatalities.

Figure 1: Posterior estimates of migrant incidents and fatalities (2014–2025). Panel (a) shows the inferred total number of incidents. Panel (b) shows the inferred total number of fatalities.

blue. Regarding incidents, the bulk of the posterior mass lies between 2,100 and 2,600. The 95% credible interval spans 2,200–2,591, implying that about 60%–71% of all incidents are captured in the MMP data. The posterior mass for fatalities falls largely between 30,000 and 40,000, with a 95% credible interval of 30,426–39,172. This translates to roughly 7–9 fatalities per day between February 17, 2014, and December 30, 2025 (compared to about 6 per day reported), suggesting that the MMP data capture approximately 66%–85% of total fatalities.

In Sec. S4 in the supplementary material, we combine these estimates with additional data and assumptions to derive mortality *rates* based on these fatality *counts*. Results suggest a likely range of 1%–3.5% per crossing attempt, reaching up to 4% in extreme cases.

We consider several robustness checks. In gray, we report alternative posterior density estimates obtained by collapsing the UN/IGO and NGO/Humanitarian lists into a single list, as these two are arguably the most similar in terms of surveillance capacity and reporting practices among the four lists considered. This allows us to assess whether the results are driven by sparse overlaps that are more likely in a four-list setting (see Tab. S3 for the corresponding three-list overlap patterns). In addition, vertical lines indicate point estimates derived from regression-based approaches following Farcomeni (2022), which we generalize to multi-list settings (see Sec. S2 in the supplementary material for details). The first regression approach utilizes a log-linear model incorporating all main effects and pairwise interactions. The second relies on model selection via AIC and BIC. The regression-based estimates generally align with the posterior density of our stratified mixture model, whereas the three-list setting yields a slightly higher incident count. For total fatalities, however, all evaluated methods demonstrate reasonably strong agreement. A dedicated prior sensitivity study suggesting that these results are robust across a range of alternative prior specifications is presented in Sec. S3 in the supplementary material. Among the 108 alternative prior settings considered there, the baseline results presented here are comparatively conservative. Farcomeni (2022) report higher observation rates than our estimates, suggesting that approximately 78% of incidents and 91% of migrant fatalities are observed under their preferred specification. However, their sample spans all borders of the European Union from January 1993 to 2019. This includes more tranquil migration periods and land border crossings, whose data availability and reporting dynamics differ fundamentally from the maritime context studied here. In addition, their analysis relies on a different methodology that neglects the

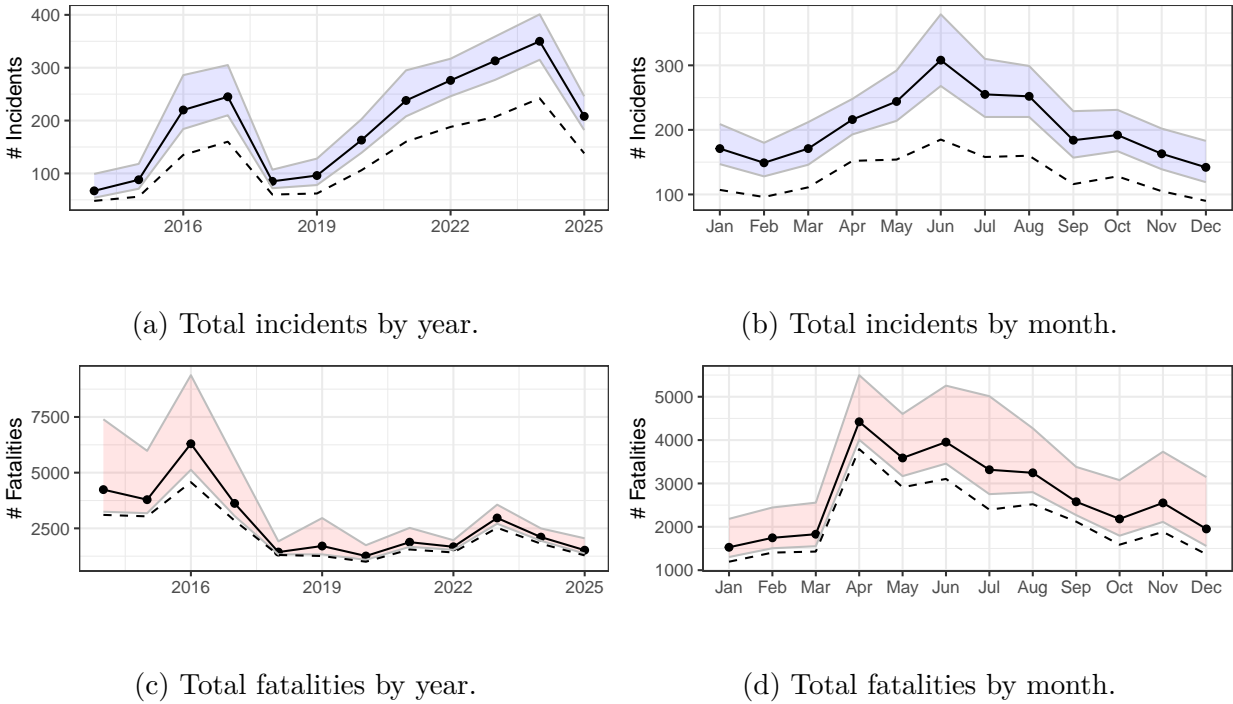
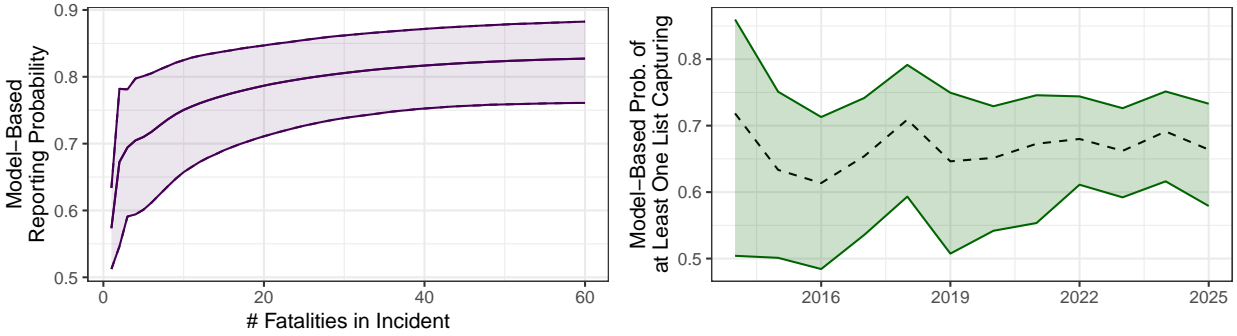


Figure 2: Posterior estimates of total incidents (top) and total fatalities (bottom), stratified by year (left) and month (right). Shaded areas are 95% credible intervals. Solid black lines are posterior medians. Dashed black lines are reported totals.

typically positive dependence between lists in their setting, which may introduce a downward bias in the hidden population estimate. Together, these substantial methodological and contextual distinctions likely explain the disparities in reported estimates.

Time-Stratified Analysis. Fig. 2 displays fatality and incident estimates stratified by year and by month. The monthly estimates are based on model runs stratified by calendar month, pooling months across years. Both levels of stratification reveal meaningful temporal variation. We find that fatalities were concentrated in the early years of the sample, especially prior to 2018. However, estimation uncertainty is also highest during these periods. This likely reflects the generally lower information content of the data during this period (see Sec. 2), together with the fact that fatality patterns become more stable after 2017, enabling greater information sharing across strata. Regarding seasonality, the majority of fatalities



(a) Probability of reporting by fatalities.

(b) Probability of reporting over time.

Figure 3: Model-implied reporting probabilities. The left panel shows the relationship between the number of fatalities per incident and the probability of reporting. The right panel displays the probability of an incident being captured by at least one list over time. In both panels, the vertical axis represents the reporting probability. Lines denote posterior medians and shaded areas indicate 95% credible intervals.

occur during the summer months. This aligns with peak crossing activity during this time of year due to favorable weather conditions (Zens & Bijak 2025). Similar temporal patterns are evident in the stratified results for incidents.

Results on Reporting Patterns and Incident Severity. Panel (a) in Fig. 3 illustrates the model-implied relationship between the number of fatalities per incident and the probability of reporting. These estimates are derived by evaluating the model-implied marginal reporting probability for specific fatality counts at each MCMC draw. We observe a distinctly positive correlation between incident severity and reporting probability. This confirms intuitive expectations regarding reporting patterns and underscores the necessity of jointly modeling reporting probabilities and fatalities in this context. Specifically, the average reporting probability for incidents with few fatalities is about 60%, whereas it increases to roughly 80–90% for larger incidents. Consequently, the undetected incidents tend to be smaller-scale with fewer fatalities. This pattern is further supported by Fig. S6, which demonstrates that

across both years and months, the observed average fatalities per incident typically fall at the upper end of the respective model-implied posterior density. Interestingly, the model-implied probability of an incident being reported by at least one list remains relatively stable over time (panel (b) of Fig. 3). However, further exploratory analyses suggest this aggregate stability may mask two diverging trends – an increasing probability of detecting large-scale events in recent years (especially since 2017; Fig. S7), counterbalanced by a steady decline in the average fatality count per incident (Fig. S3).

We additionally investigate the correlation structure between reporting and log fatalities using the fully augmented dataset (i.e., including imputed values for unobserved incidents). The resulting correlations (Fig. S8) corroborate the positive relationship between fatalities and reporting likelihood, and reveal intricate dependencies among the four reporting lists. Ultimately, these complex empirical patterns validate the need for a flexible, joint modeling framework as proposed in this article.

5 Summary, Discussion, and Concluding Remarks

Summary. This article presents a probabilistic framework for estimating migrant fatalities en route, with a specific focus on Central Mediterranean crossings. We propose a novel methodology for marked capture-recapture problems, by extending Bayesian latent class analysis to accommodate auxiliary mark data. We report three main findings. First, while recorded data successfully capture the majority of the mortality burden – approximately 66% to 85% of total fatalities and 60% to 71% of fatal incidents – a substantial share remains undocumented. Specifically, 95% credible intervals indicate approximately 4,714–13,460 unobserved fatalities and 638–1,029 unobserved incidents. Second, regarding temporal trends, the absolute number of unreported fatalities appears to be concentrated in the 2014–2016 period. Although estimated aggregate underreporting shares remain relatively stable over

time, this aggregate stability may mask more complex underlying dynamics, whereby reporting probabilities for large incidents increase while average incident size declines. Third, we find that the marginal reporting probability increases with incident severity, reflecting plausible real-world reporting behavior and underscoring the necessity of jointly modeling fatalities and reporting mechanisms in this domain.

Limitations. This study is subject to several limitations. First, as with any multiple-systems analysis method, the proposed model relies on fundamentally untestable assumptions, may suffer from identification issues, and may be sensitive to various prior choices (Manrique-Vallier et al. 2013; Aleshin-Guendel et al. 2024). We try to mitigate these concerns using estimates based on alternative modeling frameworks and prior sensitivity studies as robustness checks. Furthermore, the assumption of local independence within latent classes is an approximation. While latent classes absorb broad, common-cause drivers of co-reporting (e.g., incident severity, weather), some residual dependence between reporting channels may remain. If positive (e.g., media echoes other sources within latent classes), this dependence causes the model to overstate surveillance coverage, yielding conservative, downward-biased estimates for both unobserved incidents and total fatalities.

Second, the construction of the *meta-observer* database via recoding MMP-reported sources into distinct lists may introduce measurement error and bias. A primary concern here is incomplete recording of sources that did in fact report an incident. For example, if the MMP database systematically records only the first or first few sources associated with an event, observed overlap between lists may be biased downwards. In standard multiple-systems settings with positive list dependence, this tends to increase estimated coverage and thereby reduce the estimated hidden population, yielding conservative estimates of unobserved incidents. If this mismeasurement were unrelated to incident severity, the same logic would imply conservative estimates of total fatalities. In the present setting, however,

the direction of bias for fatality totals is not guaranteed, because source-recording errors may vary systematically with incident size and with the specific combination of lists involved. While our aggregation strategy using rather broad lists mitigates some of these issues, it ultimately does not safeguard our analyses from such biases.

Third, our study takes MMP-reported fatalities at face value. However, source-specific fatality counts can vary, especially for high-fatality incidents reliant on eyewitness accounts. The MMP reports the most conservative verified number without recording alternatives. This introduces a downward bias in the observed marks, implying that the presented total fatality estimates are lower bounds. Though outside the scope of this paper, future research could reconstruct source-specific counts for correction.

Finally, nuanced definitional issues may arise in case different sources do not define incidents and fatalities consistently over time, potentially introducing further bias. Such inconsistencies are unlikely to be substantial given the relative clarity of the target population and the unambiguous nature of death or missingness on the open sea. Nevertheless, they cannot be fully resolved without a qualitative investigation into every cited source. Future audits of the raw data and interviews with source representatives could help quantify the extent of this issue.

Future Research. Future methodological research may address some of these concerns by incorporating an additional measurement error layer into the statistical model; for instance, along the lines of joint multiple systems estimation and record linkage models ([Fienberg & Manrique-Vallier 2009](#); [Tancredi & Liseo 2011](#)). However, identification may remain challenging in the absence of a ‘gold standard’ list. Alternatively, a retrospective full source audit of captured incidents could be used to improve the robustness of the MMP data. This would, of course, be a highly resource-intensive exercise well beyond the scope of this article. Developing an objective or reference prior framework for this model class would also be

beneficial, given the typical sensitivity of capture-recapture models to prior choices. Specifying priors for overfitting mixtures of mixed binary and Gaussian data involves a delicate balance between robustness and computational stability. While we addressed this through extensive sensitivity analyses, a more principled solution regarding default priors would be a valuable theoretical contribution.

From a modeling perspective, extending the framework to incorporate smooth temporal dynamics offers a valuable refinement. Because our latent class parameters are currently shared across strata, the model inherently approximates any structural improvements in surveillance capacity as compositional shifts in incident archetypes. While this shared-parameter design ensures estimation stability, future work could allow capture probabilities to evolve continuously over time to better isolate systemic changes in reporting. Furthermore, future extensions might replace the continuous log-normal mark model with an integer-valued zero-truncated count model (e.g., overdispersed zero-truncated Poisson mixtures) to eliminate potential support-mismatch bias. However, this would come at the expense of substantially more complex posterior inference.

More broadly, working towards a more comprehensive and robust data environment is essential for accurately understanding migrant mortality and informing policy. Here, an important future research effort is to merge information contained in the MMP with auxiliary information in related databases.⁶ However, such matching exercises are far from straightforward, require extensive efforts and are beyond the scope of this study. Overall, we view this paper as an initial, methodological contribution to be used in future estimation efforts.

In conclusion, while our estimates remain contingent on incomplete data and strong modeling assumptions, they provide a principled and uncertainty-aware alternative to naive adjustment

⁶For instance, the *UNITED List of Refugee Deaths* used in [Farcomeni \(2022\)](#) is an alternative, media-focused migrant death list that provides data from 1993–2025.

rules and help clarify the likely magnitude of structural undercount. Ultimately, this work offers a foundation for improved mortality surveillance in migration contexts and paves the way for policy evaluation and monitoring. Importantly, the utility of this framework extends beyond the Central Mediterranean. It is readily applicable to other migration routes and, more broadly, to related capture-recapture settings providing auxiliary mark data, such as estimating civilian casualties in conflict or ecological surveys recording animal size.

Disclosure statement

The authors declare that they have no conflict of interest.

Acknowledgments

The authors thank Alessio Farcomeni, Anita Gohdes, Gertraud Malsiner-Walli, and the *Missing Migrants Project* team for their insightful discussions and comments that helped shape various aspects of this paper. Gregor Zens received financial support from the European Research Council (ERC) through the *2C-RISK* grant (Grant Agreement No. 101162653). Zoe Sigman received funding from the Deutsche Forschungsgemeinschaft (DFG, German Research Foundation) – 390285477/GRK 2458. Views and opinions expressed are, however, those of the author(s) only and do not necessarily reflect those of the European Union or the European Research Council Executive Agency. Neither the European Union nor the granting authority can be held responsible for them.

Data Availability Statement

The *Missing Migrants Project* data are publicly available online at <https://missingmigrants.iom.int/>. Data on attempted crossings are available online at <https://data.humdata.org/dataset/iom-missing-migrants-project-data>. The recoded dataset and the estimation and replication code are available from the authors upon request.

References

- Aleshin-Guendel, S., Sadinle, M. & Wakefield, J. (2024), ‘The central role of the identifying assumption in population size estimation’, *Biometrics* **80**(1), ujad028.
- Amstrup, S. C., McDonald, T. L. & Manly, B. F. (2010), *Handbook of capture-recapture analysis*, Princeton University Press.
- Ball, P. & Asher, J. (2002), ‘Statistics and slobodan: using data analysis and statistics in the war crimes trial of former president milosevic’, *Chance* **15**(4), 17–24.
- Ball, P., Betts, W., Scheuren, F., Dudukovich, J. & Asher, J. (2002), ‘Killings and refugee flow in kosovo march-june 1999’, *American Association for the Advancement of Science and American Bar Association’s Central and Eastern European Law Initiative, Washington, DC*.
- Bird, S. M. & King, R. (2018), ‘Multiple systems estimation (or capture-recapture estimation) to inform public policy’, *Annual Review of Statistics and Its Application* **5**(1), 95–118.
- Chan, L., Silverman, B. W. & Vincent, K. (2021), ‘Multiple systems estimation for sparse capture data: Inferential challenges when there are nonoverlapping lists’, *Journal of the American Statistical Association* **116**(535), 1297–1306.
- Chao, A. (1987), ‘Estimating the population size for capture–recapture data with unequal catchability’, *Biometrics* **43**(4), 783–791.
- Dahab, M., AbuKoura, R., Checchi, F., Ahmed, A., Abdalla, O., Ibrahim, M., Abdelmagid, N., Alabden, I. Z., Omer, L., Alhaffar, M. et al. (2025), ‘War-time mortality in sudan: a multiple systems estimation analysis’, *The Lancet Global Health* **13**(9), e1583–e1590.
- Farcomeni, A. (2022), ‘How many refugees and migrants died trying to reach Europe? Joint population size and total estimation’, *The Annals of Applied Statistics* **16**(4), 2339–2351.

- Fienberg, S. E. & Manrique-Vallier, D. (2009), ‘Integrated methodology for multiple systems estimation and record linkage using a missing data formulation’, *AStA Advances in Statistical Analysis* **93**(1), 49–60.
- Frühwirth-Schnatter, S. (2006), *Finite mixture and Markov switching models*, Springer.
- Frühwirth-Schnatter, S. & Malsiner-Walli, G. (2019), ‘From here to infinity: sparse finite versus dirichlet process mixtures in model-based clustering’, *Advances in Data Analysis and Classification* **13**(1), 33–64.
- Hagenaars, J. A. & McCutcheon, A. L. (2002), *Applied latent class analysis*, Cambridge University Press.
- International Organization for Migration (2026), ‘Missing migrants project: Tracking deaths along migratory routes’, Database. Accessed January 16, 2026.
- Johndrow, J. E., Lum, K. & Manrique-Vallier, D. (2019), ‘Low-risk population size estimates in the presence of capture heterogeneity’, *Biometrika* **106**(1), 197–210.
- Lum, K., Price, M. E. & Banks, D. (2013), ‘Applications of multiple systems estimation in human rights research’, *The American Statistician* **67**(4), 191–200.
- Lum, K., Price, M., Guberek, T. & Ball, P. (2010), ‘Measuring elusive populations with Bayesian model averaging for multiple systems estimation: A case study on lethal violations in casanare, 1998-2007’, *Statistics, Politics, and Policy* **1**(1), 2.
- Madigan, D. & York, J. C. (1997), ‘Bayesian methods for estimation of the size of a closed population’, *Biometrika* **84**(1), 19–31.
- Malsiner-Walli, G., Frühwirth-Schnatter, S. & Grün, B. (2016), ‘Model-based clustering based on sparse finite gaussian mixtures’, *Statistics and Computing* **26**(1), 303–324.

- Manrique-Vallier, D. (2016), ‘Bayesian population size estimation using dirichlet process mixtures’, *Biometrics* **72**(4), 1246–1254.
- Manrique-Vallier, D., Ball, P. & Sadinle, M. (2022), ‘Capture-recapture for casualty estimation and beyond: recent advances and research directions’, *Statistics in the Public Interest: In Memory of Stephen E. Fienberg* pp. 15–31.
- Manrique-Vallier, D., Ball, P. & Sulmont, D. (2019), ‘Estimating the number of fatal victims of the peruvian internal armed conflict, 1980-2000: an application of modern multi-list capture-recapture techniques’, *arXiv preprint arXiv:1906.04763* .
- Manrique-Vallier, D., Price, M. E. & Gohdes, A. (2013), ‘Multiple systems estimation techniques for estimating casualties in armed conflicts’, *Counting civilian casualties: An introduction to recording and estimating nonmilitary deaths in conflict* **165**.
- McLachlan, G. & Peel, D. (2000), *Finite mixture models*, John Wiley & Sons.
- Silverman, B. W. (2020), ‘Multiple-systems analysis for the quantification of modern slavery: classical and bayesian approaches’, *Journal of the Royal Statistical Society Series A: Statistics in Society* **183**(3), 691–736.
- Silverman, B. W., Chan, L. & Vincent, K. (2024), ‘Bootstrapping multiple systems estimates to account for model selection’, *Statistics and Computing* **34**(1), 44.
- Steinheilper, E. & Gruijters, R. J. (2018), ‘A contested crisis: policy narratives and empirical evidence on border deaths in the mediterranean’, *Sociology* **52**(3), 515–533.
- Tancredi, A. & Liseo, B. (2011), ‘A hierarchical bayesian approach to record linkage and population size problems¹’, *The Annals of Applied Statistics* pp. 1553–1585.
- Tanner, M. A. & Wong, W. H. (1987), ‘The calculation of posterior distributions by data augmentation’, *Journal of the American Statistical Association* **82**(398), 528–540.

Zens, G. & Bijak, J. (2025), ‘Dynamic count models with flexible innovation processes for irregular maritime migration’, *arXiv preprint arXiv:2508.18716* .

SUPPLEMENTARY MATERIAL

S1 Further MCMC Details and Derivations

In this section, we provide further details on the Gibbs sampling steps used for posterior inference. To facilitate estimation, we employ a data augmentation scheme that includes the latent cluster assignments \mathbf{z} , the number of unobserved incidents $\mathbf{n}_0 = \{n_{0g}\}_{g=1}^G$, and the latent marks for these unobserved incidents. Let the collection of all model parameters be $\Theta = \{\boldsymbol{\pi}, \mathbf{p}, \boldsymbol{\mu}, \boldsymbol{\sigma}^2, \boldsymbol{\lambda}, \boldsymbol{\alpha}\}$. For a specific stratum g , let m_g denote the number of observed incidents and n_{0g} the number of unobserved incidents. The observed data consist of reporting patterns \mathbf{s}_i and log-marks x_i for $i \in \mathcal{O}_g$. The unobserved incidents are characterized by latent log-marks $\mathbf{x}_{0g} = \{x_{0g\ell}\}_{\ell=1}^{n_{0g}}$ and are missed by all reporters, i.e. each unobserved incident has the all-zero capture pattern.

The joint probability of the data and parameters factors into an observed component and an unobserved component. Denoting the total stratum count as $N_g = m_g + n_{0g}$, the joint likelihood is proportional to

$$P(\text{Data}, \Theta) \propto P(\Theta) \times \prod_{g=1}^G \left[\frac{e^{-\lambda_g} \lambda_g^{N_g}}{N_g!} \times L_{\text{obs},g} \times L_{\text{miss},g} \right], \quad (\text{S1})$$

where $P(\Theta)$ denotes the joint prior. The contribution from the m_g observed incidents is

$$L_{\text{obs},g} = \prod_{i=1}^{m_g} \left(\sum_{k=1}^K \pi_{gk} \phi(x_i | \mu_k, \sigma_k^2) \prod_{j=1}^R p_{kj}^{s_{ij}} (1 - p_{kj})^{1-s_{ij}} \right), \quad (\text{S2})$$

and the contribution from the n_{0g} unobserved incidents is

$$L_{\text{miss},g} = \prod_{\ell=1}^{n_{0g}} \left(\sum_{k=1}^K \pi_{gk} \phi(x_{0g\ell} | \mu_k, \sigma_k^2) \prod_{j=1}^R (1 - p_{kj}) \right). \quad (\text{S3})$$

Note that the unobserved term simplifies due to the all-zero reporting patterns for unobserved incidents. Let the non-detection probability of an incident in cluster k be $q_k = \prod_{j=1}^R (1 - p_{kj})$.

S1.1 Augmenting Missing Observations

To sample the missing observations, we utilize the properties of a Poisson process under random thinning. We update the unobserved state by sampling from the joint posterior of the tuple $\{n_{0g}, \mathbf{z}_{0g}, \mathbf{x}_{0g}\}$. Conditional on the parameters Θ , this joint density is proportional to the unobserved component of the likelihood. Explicitly, we have:

$$P(n_{0g}, \mathbf{z}_{0g}, \mathbf{x}_{0g} \mid \Theta) \propto \frac{\lambda_g^{n_{0g}} e^{-\lambda_g p_{0g}}}{n_{0g}!} \prod_{\ell=1}^{n_{0g}} \left(\pi_{g, z_{0g\ell}} q_{z_{0g\ell}} \phi(x_{0g\ell} \mid \mu_{z_{0g\ell}}, \sigma_{z_{0g\ell}}^2) \right). \quad (\text{S4})$$

To sample from this joint distribution efficiently, we factorize it into a marginal distribution for the count n_{0g} and a conditional distribution for the characteristics $(\mathbf{z}_{0g}, \mathbf{x}_{0g})$ given n_{0g} . We can rewrite the term inside the product by multiplying and dividing by the marginal missing probability $p_{0g} = \sum_{k=1}^K \pi_{gk} q_k$:

$$\pi_{g, z_{0g\ell}} q_{z_{0g\ell}} \phi(x_{0g\ell} \mid \mu_{z_{0g\ell}}, \sigma_{z_{0g\ell}}^2) = p_{0g} \times \underbrace{\frac{\pi_{g, z_{0g\ell}} q_{z_{0g\ell}}}{p_{0g}}}_{P(z_{0g\ell} \mid \mathbf{s} = \mathbf{0})} \times \phi(x_{0g\ell} \mid \mu_{z_{0g\ell}}, \sigma_{z_{0g\ell}}^2). \quad (\text{S5})$$

Substituting this factorization back into the joint density expression yields:

$$P(n_{0g}, \mathbf{z}_{0g}, \mathbf{x}_{0g} \mid \cdot) \propto \frac{\lambda_g^{n_{0g}} e^{-\lambda_g p_{0g}}}{n_{0g}!} \prod_{\ell=1}^{n_{0g}} \left(p_{0g} \cdot P(z_{0g\ell} \mid \mathbf{s} = \mathbf{0}) \cdot \phi(x_{0g\ell} \mid \mu_{z_{0g\ell}}, \sigma_{z_{0g\ell}}^2) \right) \quad (\text{S6})$$

$$= \underbrace{\frac{(\lambda_g p_{0g})^{n_{0g}} e^{-\lambda_g p_{0g}}}{n_{0g}!}}_{\text{Poisson PMF for } n_{0g}} \times \prod_{\ell=1}^{n_{0g}} \underbrace{\left(P(z_{0g\ell} \mid \mathbf{s} = \mathbf{0}) \cdot \phi(x_{0g\ell} \mid \mu_{z_{0g\ell}}, \sigma_{z_{0g\ell}}^2) \right)}_{\text{i.i.d. draws for } z, x}. \quad (\text{S7})$$

This factorization justifies the following sequential sampling strategy:

1. **Update intensity.** First, update λ_g given the total count $N_g = m_g + n_{0g}$:

$$\lambda_g \sim \text{Gamma}(a_\lambda + N_g, b_\lambda + 1). \quad (\text{S8})$$

2. **Sample marginal count.** Draw the new number of unobserved incidents:

$$n_{0g} \sim \text{Poisson}(\lambda_g p_{0g}). \quad (\text{S9})$$

3. **Sample conditional characteristics.** For each of the n_{0g} incidents, draw a cluster assignment $z \sim \text{Categorical}(\mathbf{w}_g^{\text{miss}})$, where the normalized weights are $w_{gk}^{\text{miss}} = \frac{\pi_{gk} q_k}{p_{0g}}$. To arrive at the complete data used to update the model parameters, then draw a mark $x \sim \mathcal{N}(\mu_z, \sigma_z^2)$ for each of the n_{0g} incidents.

S1.2 Updating Mixture Weights and Sparsity Parameter

Let N_{gk} denote the total number of incidents (both observed and augmented) assigned to cluster k in stratum g . To improve mixing, we update the concentration parameter α_g while marginalizing out the weights $\boldsymbol{\pi}_g$. The marginal likelihood of the cluster counts $\mathbf{N}_g = (N_{g1}, \dots, N_{gK})$ under the Dirichlet-Multinomial model is:

$$P(\mathbf{N}_g | \alpha_g) \propto \frac{\Gamma(\alpha_g)}{\Gamma(\alpha_g + N_g)} \prod_{k=1}^K \frac{\Gamma(\alpha_g/K + N_{gk})}{\Gamma(\alpha_g/K)}. \quad (\text{S10})$$

We update α_g via a Metropolis-Hastings step using a random walk proposal on the log-scale, $\log(\alpha_g^*) \sim \mathcal{N}(\log(\alpha_g), \tau^2)$, where τ^2 is a tuning parameter adapted to achieve acceptance rates around 0.234. The acceptance probability for the proposal α_g^* is $\min(1, r)$, where

$$r = \frac{P(\mathbf{N}_g | \alpha_g^*) p(\alpha_g^*)}{P(\mathbf{N}_g | \alpha_g) p(\alpha_g)} \times \frac{\alpha_g^*}{\alpha_g}, \quad (\text{S11})$$

with $p(\cdot)$ denoting the Gamma prior density. The ratio α_g^*/α_g is the Jacobian correction required for the log-scale proposal. Conditional on the current α_g , we then update the weights:

$$\boldsymbol{\pi}_g | \dots \sim \text{Dirichlet} \left(\frac{\alpha_g}{K} + N_{g1}, \dots, \frac{\alpha_g}{K} + N_{gK} \right). \quad (\text{S12})$$

S2 Simulation Study

S2.1 Data Generating Processes

We study three data-generating settings for a closed population of size $N = 2500$ observed on $R = 4$ capture lists, using 200 Monte Carlo replicates per setting. All presented results are based on 250,000 retained posterior draws, obtained after discarding an initial burn-in of 25,000 iterations and thinning the remaining chain by a factor of six.

Setting A: Independence. In the simplest setup we consider, for each replicate we first generate latent marks $x_i \sim \mathcal{N}(\mu, \sigma^2)$ with $(\mu, \sigma) = (2.5, 1.0)$ for $i = 1, \dots, N$, and transform them to observed marks via $y_i = \max\{1, \text{round}(\exp(x_i))\}$. Capture indicators are then generated independently across individuals and lists as $s_{ij} \sim \text{Bernoulli}(p_j)$ with $\mathbf{p} = (0.40, 0.10, 0.12, 0.20)$ for $j = 1, \dots, 4$. Thus there is no relationship between x_i and capture, and there are no list interactions.

Setting B: Mixture (latent classes). In each replicate we generate a three-class mixture with $K = 3$ and weights $\boldsymbol{\pi} = (0.40, 0.30, 0.30)$, and class memberships are sampled from $z_i \sim \text{Categorical}(\boldsymbol{\pi})$ for $i = 1, \dots, N$. Conditional on $z_i = k$, marks are drawn as $x_i | (z_i = k) \sim \mathcal{N}(\mu_k, \sigma_k^2)$ with $\boldsymbol{\mu} = (6.0, 4.0, 2.0)$ and $\boldsymbol{\sigma} = (0.8, 0.8, 0.8)$, followed by the transformation $y_i = \max\{1, \text{round}(\exp(x_i))\}$. Given z_i , captures are independent across lists with $s_{ij} | (z_i = k) \sim \text{Bernoulli}(p_{kj})$, where

$$\begin{pmatrix} \mathbf{p}_1 \\ \mathbf{p}_2 \\ \mathbf{p}_3 \end{pmatrix} = \begin{pmatrix} 0.60 & 0.55 & 0.60 & 0.55 \\ 0.35 & 0.30 & 0.35 & 0.30 \\ 0.15 & 0.18 & 0.15 & 0.18 \end{pmatrix}.$$

The third class has both smaller marks and lower capture probabilities, inducing a positive association between severity and detectability.

Setting C: Mixture (diffuse fringe). In each replicate we generate a two-class mixture with weights $\boldsymbol{\pi} = (0.70, 0.30)$ and assignments $z_i \sim \text{Categorical}(\boldsymbol{\pi})$. Conditional on $z_i = k$, marks follow $x_i \mid (z_i = k) \sim \mathcal{N}(\mu_k, \sigma_k^2)$ with $\boldsymbol{\mu} = (4.5, 2.5)$ and $\boldsymbol{\sigma} = (0.4, 1.2)$, mapped to $y_i = \max\{1, \text{round}(\exp(x_i))\}$. Captures are conditionally independent given z_i with $s_{ij} \mid (z_i = k) \stackrel{\text{ind}}{\sim} \text{Bernoulli}(p_{kj})$ and

$$\begin{pmatrix} \mathbf{p}_1 \\ \mathbf{p}_2 \end{pmatrix} = \begin{pmatrix} 0.50 & 0.45 & 0.50 & 0.45 \\ 0.12 & 0.15 & 0.12 & 0.15 \end{pmatrix}.$$

This produces a substantial low-capture “fringe” subgroup with smaller and markedly more variable marks than the core.

S2.2 Competitor Frameworks

All competitor methods, including the Bayesian mixture model, are fit to the observed (zero-truncated) sample of size m , with observed marks y_1, \dots, y_m and capture matrix $\mathbf{S} \in \{0, 1\}^{m \times R}$. Conceptually, all competitor models use the same large-sample decomposition suggested by [Farcomeni \(2022\)](#), where the unobserved total marks can be approximated by the number of missed units times the average mark among missed units. Let $n_0 = \#\{i : \mathbf{s}_i = \mathbf{0}\}$ be the number of unobserved units, let $D_0 = \sum_{i: \mathbf{s}_i = \mathbf{0}} y_i$ be the corresponding unobserved total, and let $d_0 = \mathbb{E}[y_i \mid \mathbf{s}_i = \mathbf{0}]$ denote the mean mark for missed units. Then, as n_0 grows, the sample average mark among missed units concentrates around d_0 , so that $D_0 \approx n_0 d_0$ becomes a useful approximation; see [Farcomeni \(2022\)](#) for simulation evidence. In practice, this estimator is implemented by separately estimating \hat{n}_0 from the capture histories and \hat{d}_0 from a mark model, and reporting the plug-in estimate $\widehat{D}_0 = \hat{n}_0 \hat{d}_0$. We summarize the benchmark models we use as follows.

S2.2.1 Naive estimator (Chao).

Let $c_i = \sum_{j=1}^R s_{ij}$ denote the number of lists on which observed unit i appears, and define $f_1 = \#\{i : c_i = 1\}$ and $f_2 = \#\{i : c_i = 2\}$. The naive estimate of the number of missed units, based on [Chao \(1987\)](#), is

$$\hat{n}_0^{\text{naive}} = \frac{f_1^2}{2f_2}.$$

The mean mark among missed units is naively taken to equal the observed sample mean.,

$$\hat{d}_0^{\text{naive}} = \frac{1}{m} \sum_{i=1}^m y_i,$$

so the missed total can be estimated as

$$\hat{D}_0^{\text{naive}} = \hat{n}_0^{\text{naive}} \hat{d}_0^{\text{naive}}.$$

S2.2.2 Fixed-order regression models.

We consider first a regression-based procedure using two separate regressions; first, a model for marks to estimate \hat{d}_0 , and second, a log-linear Poisson model for capture-pattern counts to estimate \hat{n}_0 .

Mark model. For a *main effects only* mark model, we regress $\log(y_i)$ on an intercept and the four list indicators,

$$\log(y_i) = \beta_0 + \sum_{j=1}^R \beta_j s_{ij} + \varepsilon_i, \quad \varepsilon_i \sim \mathcal{N}(0, \sigma^2),$$

fit by ordinary least squares on the observed individuals. We also consider a version of the model with all *pairwise interactions*,

$$\log(y_i) = \beta_0 + \sum_{j=1}^R \beta_j s_{ij} + \sum_{1 \leq j < \ell \leq R} \beta_{j\ell} s_{ij} s_{i\ell} + \varepsilon_i.$$

The target is the expected mark for an all-zero capture history. Since all indicators (and hence all interaction products) equal zero when $s_{i1} = \dots = s_{iR} = 0$, the corresponding

predictor reduces to $\hat{\mu}_0 = \hat{\beta}_0$, and the implied mean mark is taken as the log-normal mean

$$\hat{d}_0 = \exp\left(\hat{\mu}_0 + \frac{1}{2}\hat{\sigma}^2\right),$$

where $\hat{\sigma}^2$ is the usual OLS residual variance estimate.

Event model. Let \mathbf{s}_i denote the capture pattern of observed unit i , and define pattern counts

$$n(\mathbf{s}) = \#\{i : \mathbf{s}_i = \mathbf{s}\}, \quad \mathbf{s} \in \{0, 1\}^R.$$

A Poisson GLM is fit to the $2^R - 1 = 15$ observed cells, omitting the unobserved all-zero cell $\mathbf{s} = \mathbf{0}$. Again, we consider a *main effects* only model

$$n(\mathbf{s}) \sim \text{Poisson}(\lambda(\mathbf{s})), \quad \log \lambda(\mathbf{s}) = \gamma_0 + \sum_{j=1}^R \gamma_j s_j,$$

and a model with all *pairwise interactions*

$$\log \lambda(\mathbf{s}) = \gamma_0 + \sum_{j=1}^R \gamma_j s_j + \sum_{1 \leq j < \ell \leq R} \gamma_{j\ell} s_j s_\ell.$$

The estimate of the missing all-zero cell is obtained by prediction at $\mathbf{s} = \mathbf{0}$,

$$\hat{n}_0 = \hat{\lambda}(\mathbf{0}) = \exp(\hat{\gamma}_0),$$

and the missed total is then

$$\widehat{D}_0 = \hat{n}_0 \hat{d}_0.$$

S2.2.3 Regression with model selection over hierarchical log-linear models

A second regression competitor fits a *family* of hierarchical log-linear models for both the marks regression and the incidents regression, and then selects models by AIC or BIC, computed separately for marks and incidents. For this, we treat the four lists as binary factors $L1, \dots, L4$. Candidate specifications always include all four main effects and may include any subset of the six pairwise interactions $L1:L2, \dots, L3:L4$, as well as any subset of

the four three-way interactions $L1:L2:L3$ and so on, subject to a hierarchy constraint. In total, this yields 113 possible hierarchical models.

Otherwise, the mark and event models follow the same ideas as for the regression models outlined in Sec. S2.2.2. For mark models and incident models separately, we compute AIC and BIC over the 113 candidates and select the minimizer under each criterion, yielding $(\hat{d}_0^{\text{AIC}}, \hat{n}_0^{\text{AIC}})$ and $(\hat{d}_0^{\text{BIC}}, \hat{n}_0^{\text{BIC}})$. The missed totals are reported as $\widehat{D}_0^{\text{BIC}} = \hat{n}_0^{\text{BIC}} \hat{d}_0^{\text{BIC}}$ and $\widehat{D}_0^{\text{AIC}} = \hat{n}_0^{\text{AIC}} \hat{d}_0^{\text{AIC}}$, respectively.

S2.3 Results

Table S1 summarizes the results of the simulation experiments. Unsurprisingly, the naive estimator is strongly biased and exhibits the largest error across all settings. While regression methods perform well under independence, they incur substantial bias for n_0 and D_0 under dependent data generating processes. This bias can be mitigated to some extent by employing model selection based on the BIC, consistent with considerations in Silverman (2020). The mark-augmented latent class model demonstrates high accuracy across all settings, exhibiting minimal bias and achieving the lowest RMSE overall. These performance gains are particularly evident in the mixture and fringe scenarios.

For completeness, we also evaluate the calibration of the 95% posterior credible intervals of the Bayesian model via empirical coverage across the 200 replicates. For the missing observations n_0 , we observe mild over-coverage, with empirical rates of 0.955, 0.985, and 0.960 in the independence, mixture, and fringe settings, respectively. Regarding the missing mark sum D_0 , we report empirical coverage of 0.945, 0.970, and 0.955. Overall, these results imply that the method is reasonably well-calibrated, with a slight tendency toward conservative intervals.

Table S1: Simulation Results: Bias and RMSE under three simulation settings

Model	Independence		Mixture (Latent Class)		Mixture (Fringe)		Overall	
	D_0	n_0	D_0	n_0	D_0	n_0	D_0	n_0
<i>Panel A: Average Relative Error</i>								
Naive	0.665	0.665	3.082	-0.192	0.413	-0.301	1.387	0.057
Regression (Main Effects)	0.014	0.003	-0.536	-0.595	-0.451	-0.575	-0.324	-0.389
Regression (Pairwise Interactions)	0.023	0.011	-0.560	-0.137	-0.548	-0.379	-0.362	-0.168
Regression (AIC)	0.026	0.013	-0.408	-0.002	-0.566	-0.360	-0.316	-0.116
Regression (BIC)	0.012	0.002	-0.085	-0.060	-0.358	-0.413	-0.143	-0.157
Mixture	0.001	0.002	0.049	0.013	-0.030	-0.010	0.007	0.002
<i>Panel B: Log RMSE</i>								
Naive	9.471	6.470	11.523	4.748	9.211	5.146	10.068	5.454
Regression (Main Effects)	7.731	4.350	9.837	5.801	9.282	5.765	8.950	5.305
Regression (Pairwise Interactions)	8.680	5.308	9.889	4.585	9.478	5.373	9.349	5.089
Regression (AIC)	8.323	5.294	9.844	5.310	9.554	5.495	9.241	5.366
Regression (BIC)	7.915	4.681	9.582	5.171	9.275	5.557	8.924	5.136
Mixture	7.495	4.345	8.575	4.118	8.017	4.358	8.029	4.274

Note. Results are based on 200 replicates per simulation setting. Relative error is calculated as $(\hat{x} - x_{\text{true}})/x_{\text{true}}$. For the Bayesian mixture model, point estimates correspond to posterior medians. ‘Overall’ refers to average results across the three scenarios.

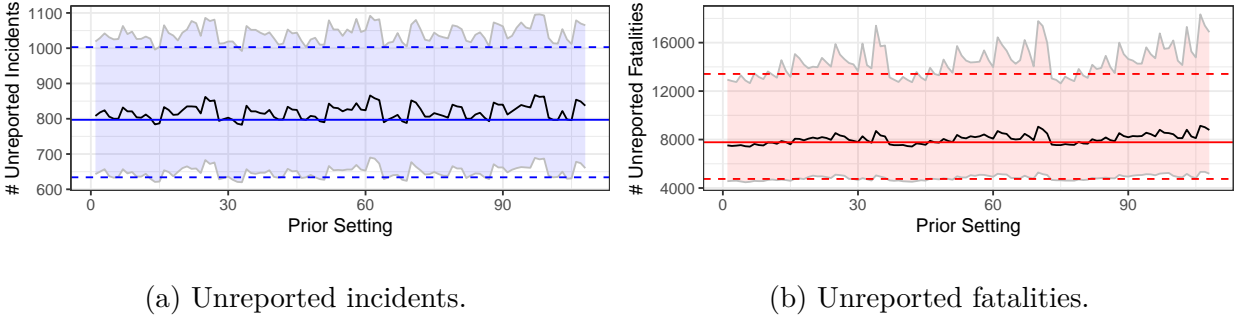


Figure S1: Prior sensitivity analysis. For each of 108 alternative prior specifications, estimated posterior median, 2.5% quantile and 97.5% quantile are shown. Horizontal lines indicate estimates under the baseline prior specification.

S3 Prior Sensitivity Analysis

Given the known sensitivity of multiple-systems estimation to parameter choices, model selection, and prior assumptions, we conduct two sets of robustness checks. First, we estimate additional regression-based models – see Sec. S2 for details – which corroborate the general location of the posterior mass from our preferred specification (see Fig. 1). Second, to investigate the influence of prior choices, we estimate our main stratified model across a total of 108 different prior specifications, all of which reflect reasonable *a priori* assumptions within a neighborhood of our baseline setup. Specifically, we vary $K \in \{80, 100, 120\}$, $c_0 \in \{3.5, 4, 4.5\}$, and $C_0 \in \{1, 1.5, 2\}$. For α_g , we consider a setting where $\alpha_g = 1$ is fixed for all g , alongside Gamma(1, 1), Gamma(1/4, 1/4), and Gamma(2, 4) priors.

The results are provided in Fig. S1. where the estimated posterior densities of missed incident and fatalities for all configurations are shown and compared to the baseline specification. We find that while there is naturally some variation in the estimates, the overall deviations remain quite small. One notable tendency is that the upper tail of the missed fatality posterior becomes slightly heavier when the prior on σ^2 is more diffuse. This is due to the heavily skewed prior predictive density implied by the log-normal distribution on the log marks x_i .

S4 Exploratory Analysis of Migrant Mortality Rates

We aim to provide an estimate of mortality *rates* for migrants using the Central Mediterranean route, complementing the fatality *counts* focused on in the main manuscript. Deriving these rates is challenging, as they are typically defined by deaths over attempted crossings. Attempted crossings are the sum of (i) successful arrivals, (ii) fatalities en route, and (iii) interceptions by North African coast guards. While (i) is measured relatively well by reception systems in Europe, components (ii) and (iii) are largely unobserved, making the denominator – and thus the mortality rate – highly uncertain. Formally, the mortality rate MR is defined as

$$\text{MR} = \frac{F}{F + A + I} = (1 - \rho) \frac{F}{A + F} \quad (\text{S13})$$

where F denotes fatalities, A denotes arrivals, I denotes interceptions and ρ represents the rate of interception (i.e., the proportion of total attempts that result in interception). We aim to recover a posterior probability distribution for MR based on this relationship. For the number of fatalities F , we rely on the posterior distribution derived from our baseline model specification. For arrivals A , we use the number of registered border crossings via the Central Mediterranean route as reported by *Frontex*.⁷

Modeling the coast guard interception rate, ρ , requires assumptions. This is not straightforward, as reliable data on interceptions are virtually nonexistent. We therefore adopt a two-scenario approach. In a first, robust scenario (‘uniform’), we remain agnostic regarding ρ , assuming it follows a uniform distribution in $[0, 1]$ for all years. In the second scenario (‘calibrated’), we calibrate a distribution for ρ based on additional data collected by the IOM.⁸ These suggest that monthly interception rates between 2016 and 2024 – after removing

⁷Available from <https://www.frontex.europa.eu/what-we-do/monitoring-and-risk-analysis/migratory-map/> (accessed Feb. 9, 2026).

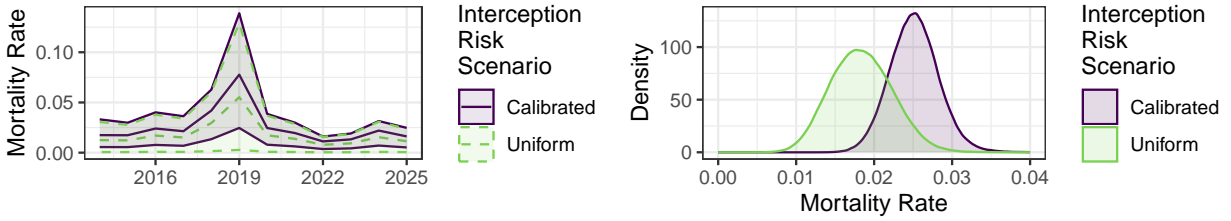
⁸Available from <https://data.humdata.org/dataset/iom-missing-migrants-project-data> (accessed Feb. 19, 2026).

outliers – vary approximately between 3% and 67%, with a mean of approximately 35%. However, these data are highly uncertain, and typically based on lower bound fatality figures. In addition, reports from North African coast guards are irregular, rarely transparent, and may suffer from reporting biases. Consequently, we assume a relatively conservative Beta(1.3, 2.8) distribution for ρ . This specification yields a median interception rate of around 32%, with approximately 95% of the probability mass falling between 2% and 77%, providing a conservative coverage of plausible values. We assume this distribution is constant across years.⁹

Based on these assumptions, we simulate mortality rates via Monte Carlo methods. We draw 250,000 samples for both ρ and F , substitute them into equation (S13), and collect the resulting samples for MR. The top panels of Fig. S2 summarize the resulting densities, both stratified by year and marginalized over time. On average, mortality rates in these scenarios fall between 1% and 3.5%. The calibrated interception scenario generally points to higher rates (between 2% and 3.5%). Estimates remain relatively stable over time, with the exception of 2019, where significantly lower arrival numbers imply a higher mortality rate; however, the wide uncertainty bounds prevent definitive conclusions regarding this spike. As a robustness check, the bottom panel of Fig. S2 reports the implied mortality rate densities for a grid of fixed values of ρ . Under the lowest-interception rate scenarios, mortality rates rise to around 4%. Overall, our simulations thus suggest that a mortality rate of up to 4% appears plausible in extreme cases.

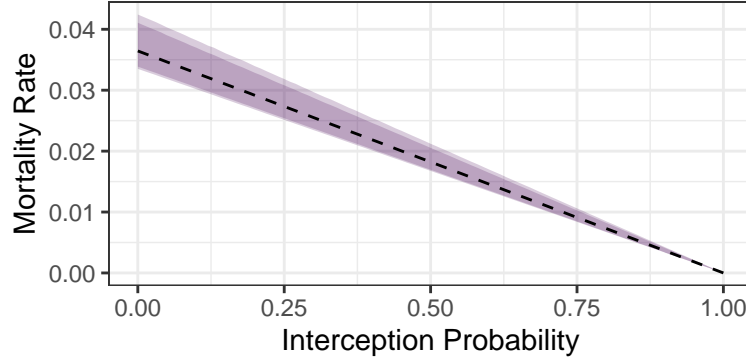
In general, this analysis should be interpreted with caution given the reliance on unverifiable assumptions and model-based estimates. Nevertheless, it is worth noting that our estimates broadly align with simpler, alternative approaches. Related literature typically estimates

⁹Interception dynamics likely shifted over time—particularly following a memorandum of understanding between Italy and Libya in 2017. Further exploratory exercises based on separate dynamics pre- and post-2017 did, however, yield comparable results. We leave a more granular temporal investigation for future work.



(a) Mortality rates by year.

(b) Marginal mortality rates.



(c) Mortality rates when varying ρ from 0 to 1.

Figure S2: Monte Carlo-based estimates of mortality rates. For top panels, interception probability is either assumed uniform or arising from a calibrated Beta distribution; see text for details. Bottom panel shows estimates based on a grid of fixed values for ρ . Point estimates refer to the posterior median. Shaded areas are 2.5% and 97.5% quantiles.

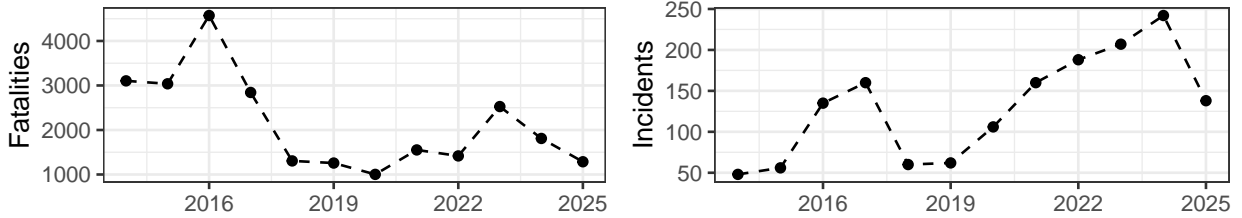
rates of similar magnitude, ranging from 0.3% to 1.8%¹⁰ or, in direct IOM estimates,¹¹ averaging around 2.8% with a similar observed increase in 2019. [Steinhilper & Gruijters \(2018\)](#) report a point estimate of 0.875% for *all* Mediterranean irregular migration routes for the period 2009-2016, ignoring coast guard interceptions. Note that the analysis presented here applies only to the Central Mediterranean Route and only for the years 2014–2025. It should not be interpreted as applying to other routes or time periods.

¹⁰See https://www.bertelsmann-stiftung.de/fileadmin/files/Projekte/Migration_fair_gestalten/IB_PolicyBrief_2018_06_Asyllum_Centers.pdf (accessed Feb. 9, 2026).

¹¹<https://publications.iom.int/system/files/pdf/mortality-rates.pdf> (accessed Feb. 9, 2026).

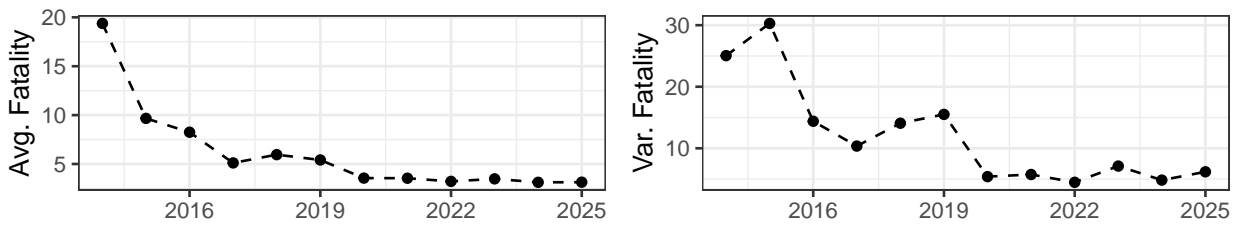
S5 Further Results

S5.1 Additional Figures



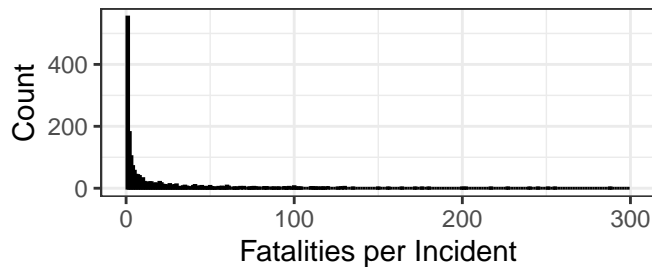
(a) Total fatalities.

(b) Total incidents.



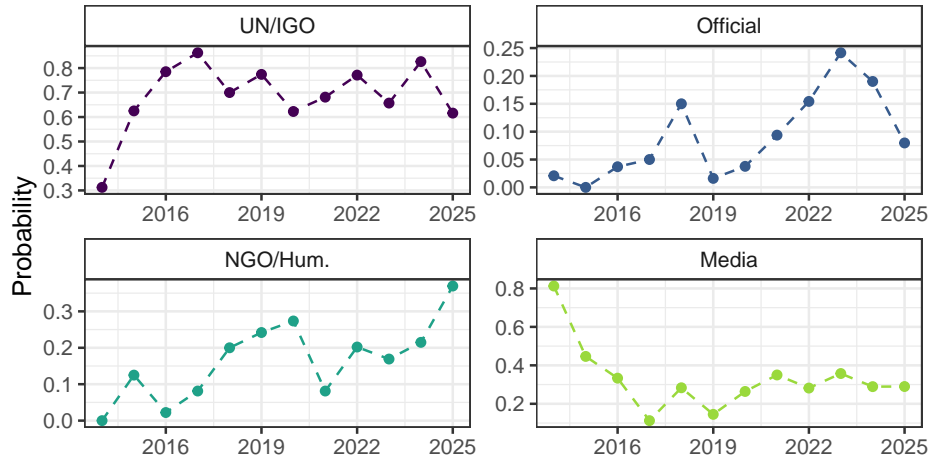
(c) Mean fatalities per incident.

(d) Variance of fatalities per incident.

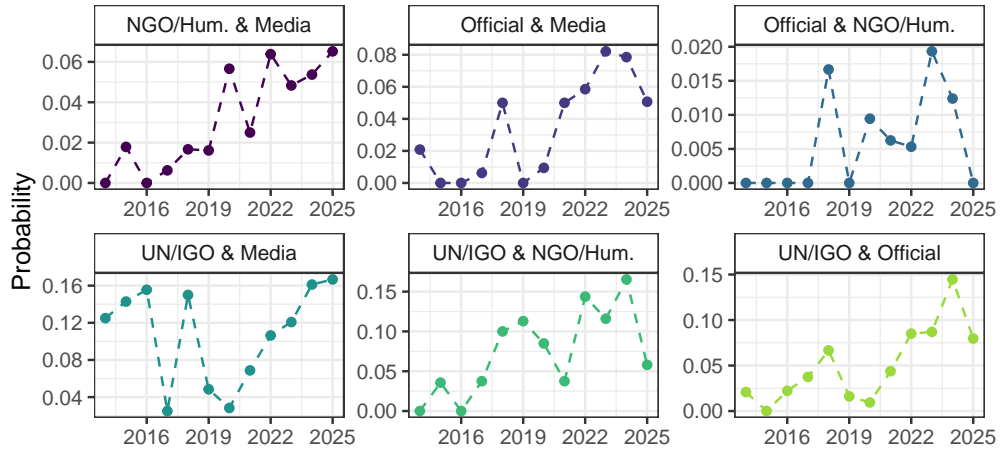


(e) Fatalities per incident.

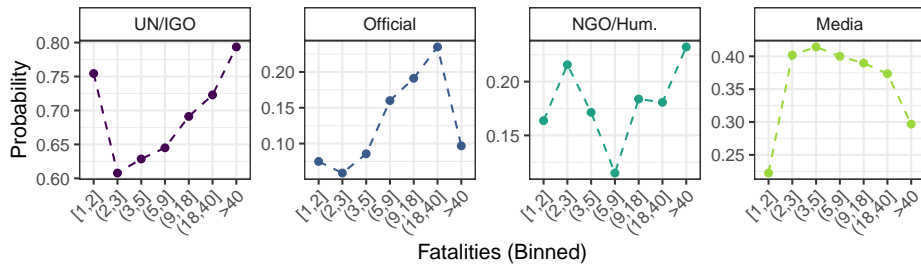
Figure S3: Panels (a) and (b) show total fatalities and incidents over time. Panels (c) and (d) track the sample mean and variance of fatalities over time. Panel (e) shows a histogram of fatalities per incident, omitting eight high fatality incidents for visualization purposes.



(a) Marginal reporting by list.

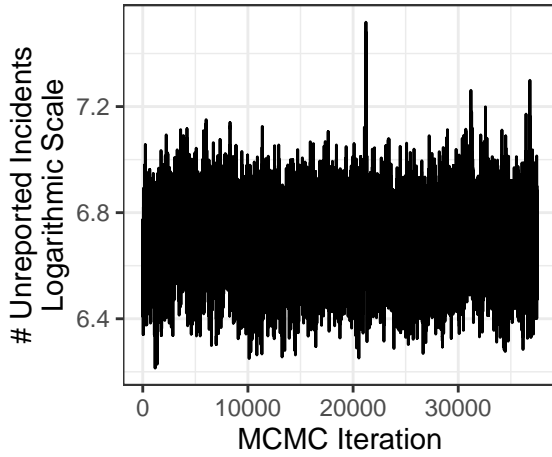


(b) Pairwise reporting by list pair.

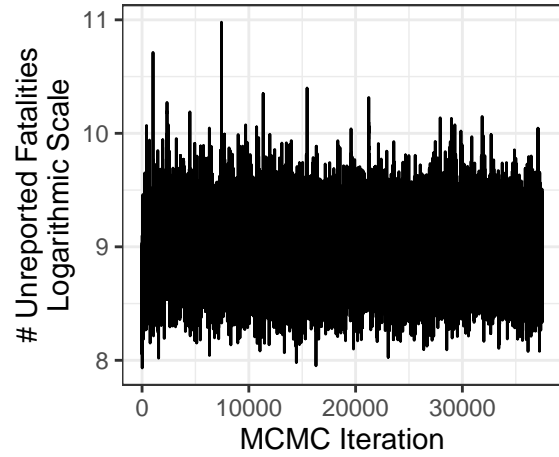


(c) Reporting by incident severity.

Figure S4: Panel (a) shows marginal reporting patterns by list. Panel (b) shows pairwise reporting patterns for list pairs. Panel (c) shows reporting patterns as a function of fatalities. The x -axis displays fatality bins based on deciles of the empirical fatality distribution. Figures are based on observed data sample and are conditional on an incident being observed.

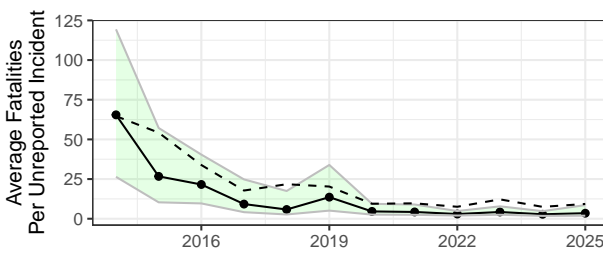


(a) Log Missing Incidents.

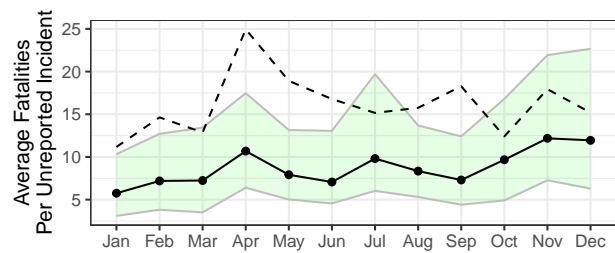


(b) Log Missing Fatalities.

Figure S5: MCMC trace plots under the baseline year-stratified specification.



(a) Expected fatalities (by year).



(b) Expected fatalities (by month).

Figure S6: Posterior densities of expected fatality count for unobserved incidents by year (left) and by month (right). The dashed line shows the mean fatality count among reported incidents. Shaded bands indicate 95% credible intervals. Solid line is posterior median.

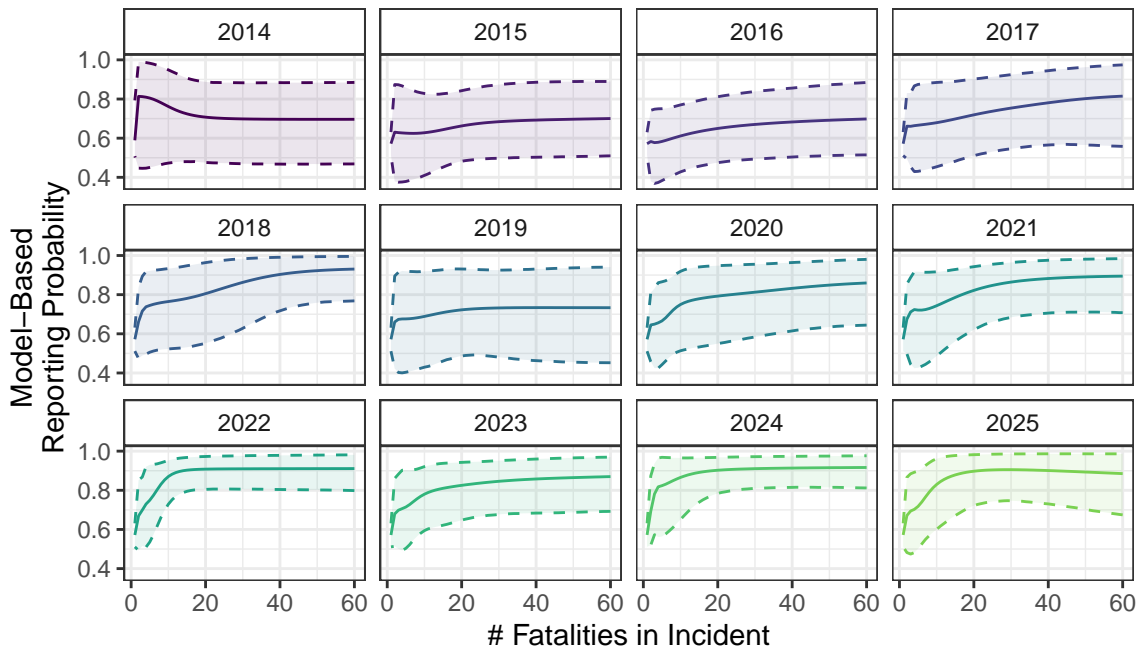


Figure S7: Model-based probability of an incident being reported (y -axis) as a function of fatalities in incident (x -axis) over years (panels). Dashed lines are posterior mean estimates, solid lines are 95% credible intervals.

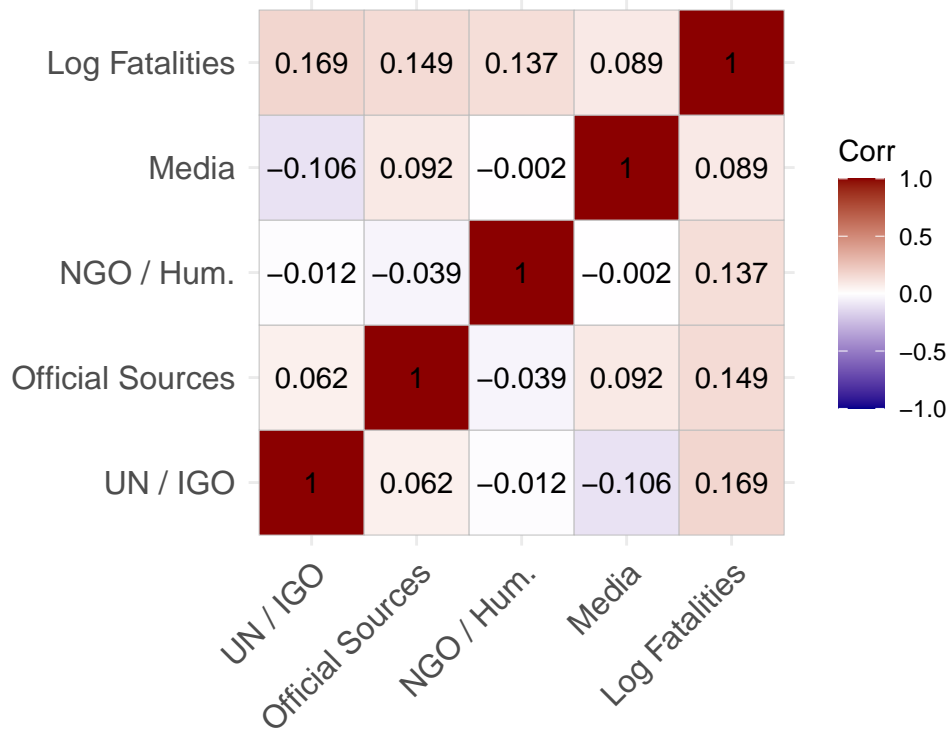


Figure S8: Posterior mean estimate of raw correlation matrix of reporting patterns s_i and log fatalities x_i , based on complete data (including imputed values for unobserved incidents). Results are averaged across years.

S5.2 Additional Tables

Table S2: List Overlap Patterns (Four Lists).

UN/IGO	Official	NGO/Hum.	Media	Count
•				771
	•			35
		•		97
			•	236
•	•			72
•		•		109
•			•	119
	•	•		3
	•		•	33
		•	•	28
•	•	•		1
•	•		•	28
•		•	•	23
	•	•	•	5
•	•	•	•	2
<i>Total</i>				1,562

Note: Each row represents a unique capture pattern across the four data sources. ‘•’ indicates inclusion in the respective list. Count refers to the number of records observed in each overlap pattern. UN/IGO = United Nations/Intergovernmental Organizations; NGO/Hum. = Non-Governmental Organizations/Humanitarian sources.

Table S3: List Overlap Patterns (Three Lists).

UN/IGO/NGO/Hum.	Official	Media	Count
•			977
	•		35
		•	236
•	•		76
•		•	170
	•	•	33
•	•	•	35
<i>Total</i>			1,562

Note: Each row represents a unique capture pattern across the three data sources. ‘•’ indicates inclusion in the respective list. Count refers to the number of records observed in each overlap pattern. UN/IGO/NGO/Hum = United Nations/Intergovernmental Organizations/Non-Governmental Organizations/Humanitarian sources.